SYNTHESIS AND PHOTOCATALYTIC STUDIES OF ZnO NANOPARTICLES

Thesis submitted as a partial fulfillment for award of the degree of Masters of Science in Physics

Submitted by

Neeraj Mittal

M.Sc. (Physics) 2nd Yr

(300804017)

Under the guidance of

Dr. O.P. Pandey

Professor & Head

School of Physics and Materials Science

THAPAR UNIVERSITY

PATIALA

CERTIFICATE

This is to certify that Miss Neeraj Mittal, Roll No. 300804017 has worked on this thesis report as a final fulfillment for award of the degree of MASTERS OF SCIENCE in Physics. I certify that the matter embodied in this report is of the candidate's own record and not submitted to any other university in any part or full form for the award of such kind of a degree.

Prof. O. P. Pandey
Supervisor
&
Head
School of Physics and Materials Science
Thapar University
Patiala

Prof. R. K. Sharma
Dean of Academic Affairs
Thapar University
Patiala

ACKNOWLEDGEMENT

"The real spirit of achieving a goal is through the way of excellence and discipline"

I would have never succeeded in completing my task without the cooperation, encouragement and help provided to me by various personalities. First of all I render my gratitude to ALMIGHTY who bestowed self confidence, ability and strength in me to complete this work.

With deep sense of gratitude I express my sincere thanks to esteemed and worthy supervisor Dr. O.P.Pandey, Professor and Head School of Physics and Materials Science for his valuable guidance in carrying out this work under his effective supervision, encouragement, enlightenment and cooperation. I shall be failing in my duties if I do not express my deep sense of gratitude towards him because he has been a source of inspiration for me in this work.

My special thanks to Mr. Manoj Sharma, Mr. Purushottam Singh, Mr. Paramjyot Kumar Jha for their timely help, cooperation, useful discussions and good wishes.

I owe my sincere thanks to Dr. Susheel Mittal, Mr. Dinesh Kumar from Chemistry department, all the faculty and staff members of School of Physics and Materials Science for their support and encouragement. I would also like to thank my friends especially Jagdeep Kaur who helped me during my work.

My project would have not seen daylight without the immense cooperation and moral support of my parents who kept my spirits up during the endeavor.

Great thaks to all my well wishers

(Neeraj Mittal)

CONTENTS

ABSTRACT

This thesis focuses on the size controlled ZnO semiconductor nanoparticles synthesized via chemical precipitation method, also covering the characterization, optical properties and photocatalytic activity of these NPs for dye degradation. Three parts mainly involved in this work are synthesis TG (1%, 2%) capped ZnO NPs, ME (1%, 2%) capped ZnO NPs and uncapped ZnO NPs. We used various experimental techniques for the measurement of size and band gap of these NPs. The techniques used are X-Ray Diffraction (XRD), UV Visible, Scanning electron microscopy (SEM) and photoluminescence. To check the presence of various elements we used EDX also. The XRD patterns of these sample revealed that the required phase is present with a little amount of impurities. The particle size measurement was done by the XRD Scherer's formula. UV Visible revealed that the required band gap has been attained. SEM micrographs showed no more agglomeration. EDX confirmed the presence of both Zn and O and photoluminescence proved the optical properties of these NPs. The measurements using above techniques have proven the NPs to be useful for the photocatalytic degradation of dye. The sample used for this activity was the TG (2%) capped ZnO because of having maximum band gap out of all prepared samples which was observed by UV Visible spectroscopy. The dye taken under experiment was crystal violet. The time of 2 hours and 20 min was taken to break the dye. With time the absorbance of dye decreased and finally when the dye became colorless we concluded that it has been broken.

Chapter - 1

Introduction

1.1 History of nanotechnology:

The first concepts found in 'nano-technology' was “There's Plenty of Rooms at the Bottom" given by physicist Richard Feynman at an American Physical Society meeting at Caltech on December 29, 1959. But the earliest nano-sized objects known to us were made of gold [1]. Faraday prepared colloidal gold in 1856 and called it ‘divided metals’. In 1974 Taniguchi approached nanotechnology from the 'top-down' standpoint and K. Eric Drexler explored the basic idea in much more depth and introduced the term "nanotechnology" more precisely in 1986, using it to describe a 'bottom-up' approach. Nanotechnology and nanoscience got started in the early 1980s with two major developments; the birth of cluster science and the invention of the scanning tunneling microscope (STM). This development led to the discovery of carbon nanotubes a few years later. In another development, the synthesis and properties of semiconductor nanocrystals was studied; this led to a fast increasing number of metal and metal oxide nanoparticles .The atomic force microscope was invented six years after the STM was invented. In year 2000, the United States National Nanotechnology Initiative was founded to coordinate Federal nanotechnology research and development.

1.2 Nanotechnology:

Nanotechnology is the understanding and control of matter at dimensions of roughly 1 to 100 nanometers [1]. It is the act of purposefully manipulating matter at the atomic scale, otherwise known as the "Nanoscale”. The future, "nanotechnology" will likely include building machines and mechanisms with nanoscale dimensions.

1.3 Nanoscale:

It uses a basic unit of measurement called a "nanometer" (abbreviated nm). There are one billion nm to a meter [1]. Each nm is only three to five atoms wide. They're small, really small ~40,000 times smaller than the width of an average human hair. A nanometer is one thousandth of a micron, and a thousandth of a millionth of a meter as shown in fig. 1.1. [2]. Another way to

visualize a nanometer is like 1 inch = 25,400,000 nanometers and red blood cells are ~7,000 nm in diameter, and ~2000 nm in height.

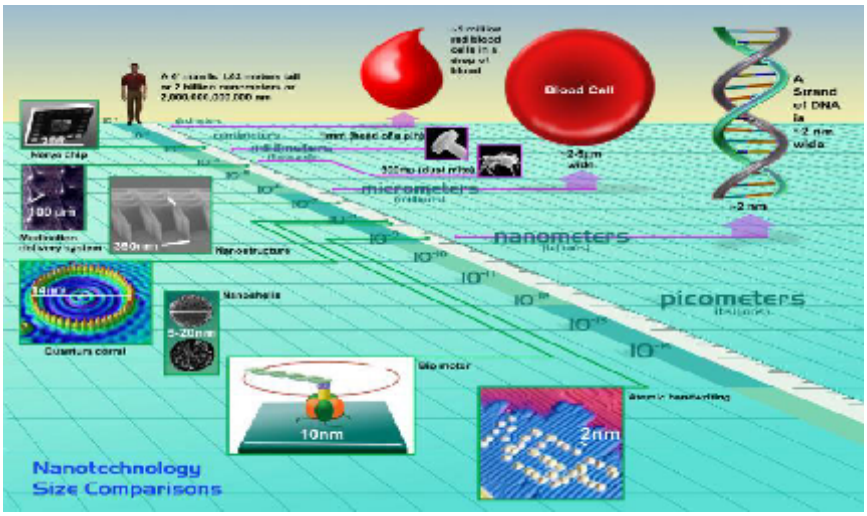

Fig. 1.1 Demonstration of Nanoscale [2]

1.4 Nanoparticles:

There is no accepted international definition of a nanoparticle, but one given in the UK is: "A particle having one or more dimensions of the order of 100nm or less". In nanotechnology a particle is defined as a small object that behaves as a whole unit in terms of its transport and properties [1]. It is further classified according to size: in terms of diameter fine particles cover a range between 100 and 2500 nanometers while ultrafine particles, on the other hand, are sized between 1 and 100 nanometers. Similar to ultrafine particles, nanoparticles are sized between 1 and 100 nanometers. The properties that differentiate the nanoparticles from the bulk material typically develop at a critical length of under 100nm. Nanoparticles may or may not exhibit size-related properties that differ significantly from those observed in fine particles or bulk materials. Although the size of most molecules would fit into the above outline, individual molecules are usually not referred to as nanoparticles.

1.5 TYPES OF NANOMATERIALS:

1.5.1 Zero dimensional nanoparticles:

The particles which are confined in all the three spatial dimensions and posses properties that are between the properties of bulk semiconductors and those of discrete molecules [3].

Quantum dots: Also known as nanocrystals shown below in fig. 1.2 (a) [4] and 1.2 (b) [5] are nanosized semiconductors that, depending on their size, can emit light in all colors of the rainbow. These nanostructures confine conduction band electrons, valence band holes, or excitons in all three spacial directions. Examples of quantum dots are semiconductor nanocrystals and core-shell nanocrystals, where there is an interface between different semiconductor materials. They have been applied in biotechnology for cell labeling and imaging, particularly in cancer imaging studies. A quantum dot for a semiconductor is whose excitons are confined in all three spatial dimensions. As a result, they have properties that are between those of bulk semiconductors and those of discrete molecules.

Fig. 1.2 (a) Quantum dots

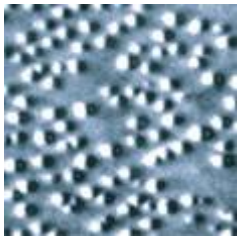

Fig. 1.2 (b) Quantum dots

1.5.2 One dimensional nanomaterial:

These substances are confined in two spatial dimensions [6].

Nanowires: A nanowire is a nanostructure, with the diameter of the order of a nanometer (10^{-9} meters). The structure of nanowires of different materials is shown in fig. 1.3 (a) [7], fig. 1.3 (b) [8] and fig. 1.3 (c) [9]. Alternatively, nanowires can be defined as structures that have a thickness or diameter constrained to tens of nanometers or less. At these scales, quantum mechanical effects are important which coined the term "quantum wires". The nanowires could be used, in the near future, to link tiny components into extremely small circuits. Using nanotechnology, such components could be created out of chemical compounds.

Fig. 1.3 (a) [7]

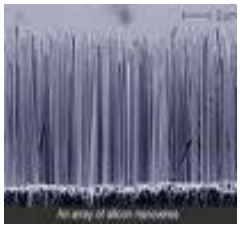

Fig. 1.3 (b) [8]

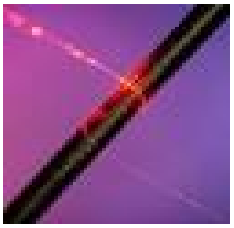

Fig. 1.3 (c) [9]

1.5.3 Two dimensional nanoparticles:

These substances are confined in only one spatial dimension.

Nanotubes: The most important nanotubes are carbon nanotubes. Carbon tubes are carbon based lattice-like, potentially porous molecules. These are cylindrical. The diameter of a carbon tube can be several nm but the length can be much greater, up to several mm [10]. Carbon tubes have many applications in materials science due to their strength and unique electrical properties. However, they have also found use in the field of biomedicine as carriers for vaccines, drugs and other molecules. A single wall carbon tube is a one-atom-thick sheet of graphite, resembling chicken wire, rolled seamlessly into a tube as shown in fig. 1.4 (a) [11]. There are also multi-walled and other types of tubes shown in fig. 1.4 (b).

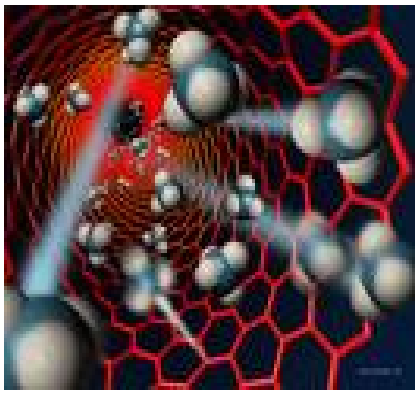

Single walled nanotubes

Fig. 1.4 (a) [11]

Double walled nanotubes

Fig. 1.4 (b) [10]

1.6 Properties of nanoparticles:

Nanoparticles act as a bridge between bulk material and atomic or molecular structures. A bulk material possesses constant physical properties regardless of its size but at the nano-scale. This is

often not the case where size-dependent properties are often observed. Thus, the properties of materials change as their size approaches the nanoscale and as the percentage of atoms at the surface of a material becomes significant. For bulk materials larger than one micrometer (or micron), the percentage of atoms at the surface is insignificant in relation to the number of atoms in the bulk of the material. The interesting and sometimes unexpected properties of nanoparticles are therefore largely due to the large surface area of the material, which dominates the contributions made by the small bulk of the material. Some key observations are as below:

- Exhibit high solar radiation absorption as compare to bulk material or sheets.
- They are super hard materials that do not exhibit the same malleability and ductility as bulk material, e.g. cooper nanoparticles smaller than 50nm.
- Possesses high electrical conductivity [1].
- Often possess unexpected optical properties as they are small enough to confine their electrons and produce quantum effects. For example gold nanoparticles appear deep red to black in solution.
- Interaction with other particles gets changed. It becomes strong enough to overcome the density differences.
- Have the property of UV blocking so they are used in sunscreen lotions.e.g. ZnO.
- They are attached to textile fibers in order to create smart and functional clothing because they increase the reinforcement when incorporated into the polymers e.g. clay nanoparticles.
- Ferroelectric materials smaller than 10 nm can switch their magnetization direction using room temperature thermal energy, thus making them unsuitable for memory storage.
- Band gap changes with change in scale.

1.7 What is different about a nanoparticle:

There is no strict dividing line between nanoparticles and non-nanoparticles. The size at which materials display different properties to the bulk material is material dependant and can certainly be claimed for many materials much larger in size than 100nm. Definitions certainly become more difficult for materials that are a very long way from being a sphere, such as carbon nanotubes [12]. One of the aims for these materials is to grow them into long tubes, certainly not

'nano' in length, but as they have a diameter in the order of 3nm for a single walled tube, they have properties that distinguish them from other allotropes of carbon, and hence can be described as 'nanomaterials'. This sort of nanomaterial has led to the extension of the idea of nanomaterials being considered as such if any one of their structural features is on a scale of less than 100nm, that cause their properties to be different from that of the bulk material.

1.8 Why nanoparticles exhibit such properties:

1.8.1 Quantum confinement:

Quantum confinement is a very successful model for describing the size dependent electronic structure of nanometer sized semiconductor structures [1]. Generally speaking, it predicts increasing band gaps with decreasing particle sizes due to shifting of the band edges. The majority of theoretical investigations on quantum confinement effects were performed on isolated particles with idealized structures and surface terminations. The quantum confinement effect can be observed once the diameter of the particle is of the magnitude as the wavelength of electron wave function [1]. When the materials are so small, their electronic and optical properties deviate substantially from those of bulk materials. A particle behaves as if it were free when the confining dimension is large compared to the wavelength of the particle. During this state, band gap remains at its original energy due to continuous energy state. However, as the confining dimension decreases and reaches a certain limit, typically in nanoscale, the energy spectrum turns to discrete as it is shown below in fig. 1.5 [13]. As a result, bandgap becomes size dependent. This ultimately results a blue shift in optical illumination as the size of the particles decreases. Specifically, the effect describes the phenomenon that results from electrons and electron holes being squeezed into a dimension that approaches a critical quantum measurement, called the excitons Bohr radius. In current application, a quantum dot confines in all three dimensions such as a small sphere, a quantum wire confines in two dimensions, and a quantum well confines in one dimension.

1.8.2 Surface to volume ratio (SA/V):

It plays a very important role in technology. As the surface area increases the complete term increases but the volume remains same. Nanostructures & nanomaterials possess a large fraction

of surface atoms per unit volume. The ratio of surface atoms to interior atoms changes dramatically if one successively divides a macroscopic object into smaller parts [1]. Such a drastic increase in the ratio of surface atoms to interior atoms in nanostructures and nanomaterials might illustrate why changes in size range of nanometers are expected to lead to great changes in physical and chemical properties of the material. As the scale decreases (keeping the volume constant) the surface area of the material increases as shown in fig. 1.6 [14] and with increases in surface area the ability of the particles to interact with other particle increases. Also the physical and chemical properties like interactive forces, reactivity etc. increases. So the SA/V ratio has a significant impact on the properties of nanoparticles.

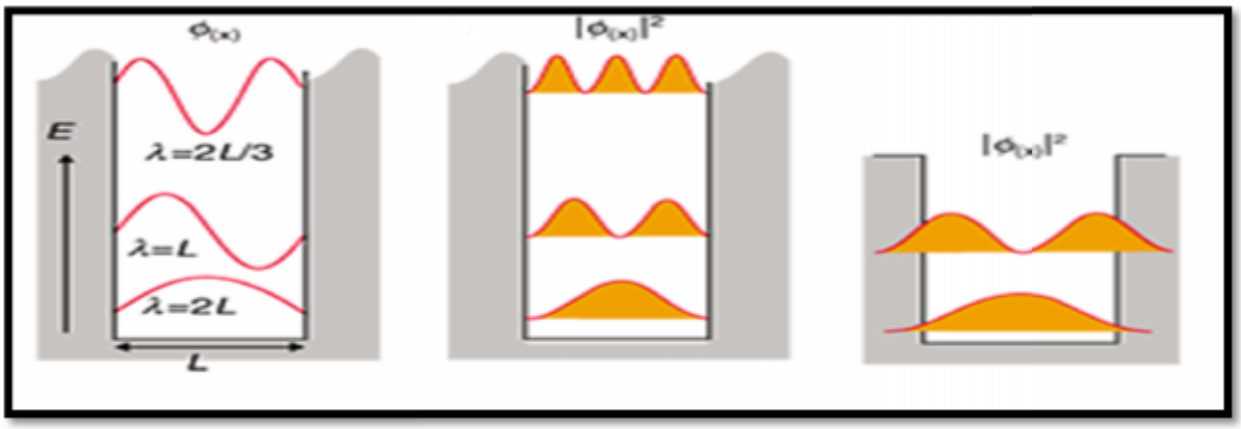

Fig. 1.5 Representation of quantum confinement [13]

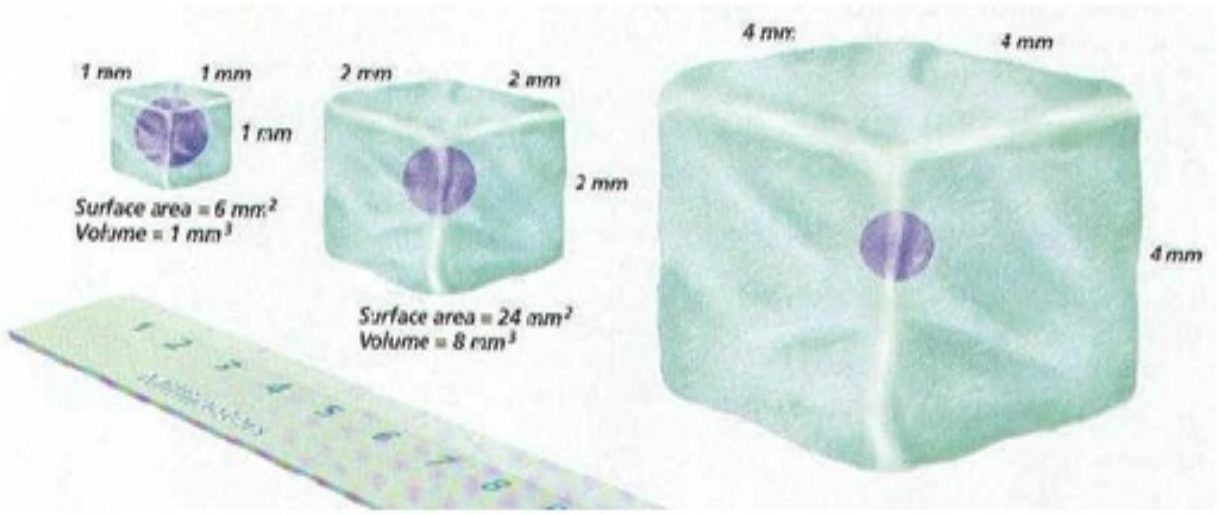

Fig. 1.6 Representation of surface to volume ratio [14]

1.8.3 Brownian motion:

Brownian motion is characterized by the constant and erratic movement of minute particles in a liquid or gas. The molecules that make up the fluid, in which the particles are suspended, as a result of the inherently random nature of their motions, collide with the larger suspended particles at random, making them move, in turn, also randomly. At macroscale we barely see the movement of particles or why they move but at nanoscale the particle moves wildly batted about by a smaller particle.

1.9 Applications of nanoparticles:

1.9.1 Medicine:

The size of nanomaterials is similar to that of most biological molecules and structures; therefore, nanomaterials can be useful for both in vivo and in vitro biomedical research and applications. Thus far, the integration of nanomaterials with biology has led to the development of diagnostic devices, contrast agents, analytical tools, physical therapy applications, and drug delivery vehicles [1].

1.9.2 Diagnostics:

Magnetic nanoparticles, bound to a suitable antibody, are used to label specific molecules, structures or microorganisms. Gold nanoparticles tagged with short segments of DNA can be used for detection of genetic sequence in a sample. Multicolor optical coding for biological assays has been achieved by embedding different-sized quantum dots into polymeric microbeads [1]. Nanopore technology for analysis of nucleic acids converts strings of nucleotides directly into electronic signatures.

1.9.3 Drug delivery:

The overall drug consumption and side-effects can be lowered significantly by depositing the active agent in the morbid region only and in no higher dose than needed. This highly selective approach reduces costs and human suffering. An example can be found in dendrimers and nanoporous materials [1]. They could hold small drug molecules transporting them to the desired

location. Some potentially important applications include cancer treatment with iron nanoparticles or gold shells. A targeted or personalized medicine reduces the drug consumption and treatment expenses resulting in an overall societal benefit by reducing the costs to the public health system. Nanotechnology is also opening up new opportunities in implantable delivery systems, which are often preferable to the use of injectable drugs, because the latter frequently display first-order kinetics (the blood concentration goes up rapidly, but drops exponentially over time). This rapid rise may cause difficulties with toxicity, and drug efficacy can diminish as the drug concentration falls below the targeted range.

1.9.4 Tissue engineering:

Nanotechnology can help to reproduce or to repair damaged tissue. “Tissue engineering” makes use of artificially stimulated cell proliferation by using suitable nanomaterial-based scaffolds and growth factors. Tissue engineering might replace today’s conventional treatments like organ transplants or artificial implants [1]. Advanced forms of tissue engineering may lead to life extension.

For patients with end-state organ failure, there may not be enough healthy cells for expansion and transplantation into the ECM (extracellular matrix). In this case, pluripotent stem cells are needed. One potential source for these cells is IPS (induced Pluripontent Stem cells); these are the ordinary cells from the patient’s own body that are reprogrammed into a pluripotent state, and has the advantage of avoiding rejection (and the potentially life-threatening complications associated with immunosuppressive treatments).

1.9.5 Chemistry and environment:

Chemical catalysis and filtration techniques are two prominent examples where nanotechnology already plays a role. The synthesis provides novel materials with tailored features and chemical properties: for example, nanoparticles with a distinct chemical surrounding (ligands), or specific optical properties. In this sense, chemistry is indeed a basic nanoscience.

1.9.6 Catalysis:

Chemical catalysis benefits especially from nanoparticles, due to the extremely large surface to volume ratio. The application potential of nanoparticles in catalysis ranges from fuel cell to catalytic converters and photocatalytic devices. Catalysis is also important for the production of chemicals. Platinum nanoparticles are now being considered in the next generation of automotive catalytic converters because the very high surface area of nanoparticles could reduce the amount of platinum required [1].

1.9.7 Filtration:

A strong influence of nanochemistry on waste-water treatment, air purification and energy storage devices is to be expected. Mechanical or chemical methods can be used for effective filtration techniques. One class of filtration techniques is based on the use of membranes with suitable hole sizes, whereby the liquid is pressed through the membrane. Nanoporous membranes are suitable for a mechanical filtration with extremely small pores smaller than 10 nm ("nanofiltration") and may be composed of nanotubes. Nanofiltration is mainly used for the removal of ions or the separation of different fluids. On a larger scale, the membrane filtration technique is named ultrafiltration, which works down to between 10 and 100 nm.

1.9.8 Increasing the efficiency of energy production:

Today's best solar cells have layers of several different semiconductors stacked together to absorb light at different energies but they still only manage to use 40 percent of the Sun's energy. Commercially available solar cells have much lower efficiencies (15-20%). Nanotechnology could help increase the efficiency of light conversion by using nanostructures with a continuum of bandgaps. Nanotechnology could improve combustion by designing specific catalysts with maximized surface area. In 2005, scientists at the University of Toronto developed a spray-on nanoparticle substance that, when applied to a surface, instantly transforms it into a solar collector.

1.9.9 Displays:

The production of displays with low energy consumption could be accomplished using carbon nanotubes (CNT). Carbon nanotubes are electrically conductive and due to their small diameter of several nanometers, they can be used as field emitters with extremely high efficiency for field emission displays (FED).

1.9.10 Optics:

The first sunglasses using protective and anti-reflective ultrathin polymer coatings are on the market. For optics, nanotechnology also offers scratch resistant surface coatings based on nanocomposites. Nano-optics could allow for an increase in precision of pupil repair and other types of laser eye surgery.

1.9.11 Cosmetics:

One field of application is in sunscreens. The traditional chemical UV protection approach suffers from its poor long-term stability. A sunscreen based on mineral nanoparticles such as titanium dioxide offer several advantages [1]. Titanium oxide nanoparticles have a comparable UV protection property as the bulk material, but lose the cosmetically undesirable whitening as the particle size is decreased.

1.10 Fabrication methods of nanoparticles:

There are wide variety of techniques that are capable of creating nanostructures with various degrees of quality, cost and speed. These manufacturing techniques fall under two categories ‘bottom-up’ and ‘top-down’. In recent years the limits of each approach, in terms of feature size and quality that can be achieved, have started to converge [15]. A diagram that illustrates the types of materials and products that these two approaches used for is shown below:

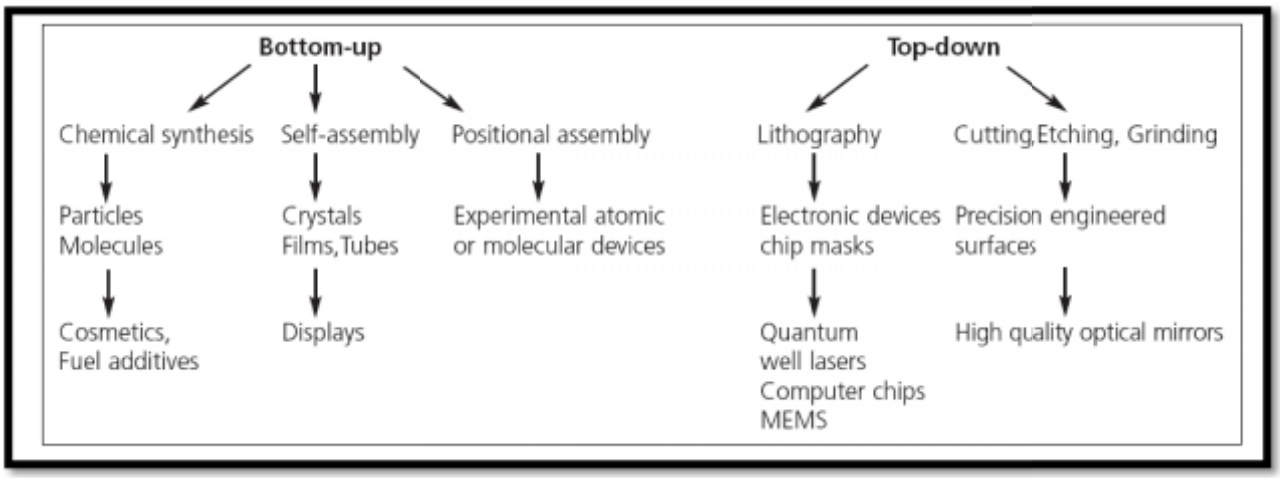

1.11 CHARACTERISATION TECHNIQUES:

1.11.1 Transmission electron microscopy:

The transmission electron microscope (TEM) is a scientific instrument that uses electrons instead of light to scrutinize objects at very fine resolutions [1]. They were developed in the 1930s when scientists realized that electrons can be used instead of light to "magnify" objects or specimens under study. Electron microscopes use electrons instead of photons, because electrons have a much shorter wavelength than photons and so allows you to observe matter with atomic resolution [1]. Transmission Electron Microscope (TEM) shoots electrons through the sample and measures how the electron beam changes because it is scattered in the sample.

Components of TEM:

1. Vacuum system 2. Specimen stage 3. Electron gun 4. Electron lens 5. Apertures.

All these components are shown below in fig. 1.7 [16].

Imaging methods: Imaging methods in TEM utilize the information contained in the electron waves exiting from the sample to form an image. The projector lenses allow for the correct positioning of this electron wave distribution onto the viewing system.

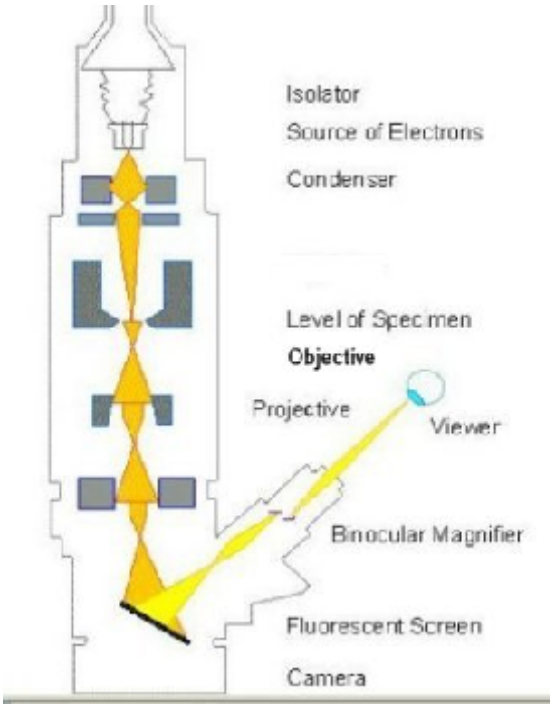

Fig. 1.7 Experimental set-up for TEM [16]

.

Bright field: The most common mode of operation for a TEM is the bright field imaging mode. In this mode the contrast formation, when considered classically, is formed directly by occlusion and absorption of electrons in the sample [1]. Thicker regions of the sample, or regions with a higher atomic number will appear dark, whilst regions with no sample in the beam path will appear bright – hence the term "bright field".

Diffraction contrast: Samples can exhibit diffraction contrast, whereby the electron beam undergoes Bragg scattering, which in the case of a crystalline sample, disperses electrons into discrete locations in the back focal plane. By the placement of apertures in the back focal plane, i.e. the objective aperture, the desired Bragg reflections can be selected (or excluded), thus only parts of the sample that are causing the electrons to scatter to the selected reflections will end up projected onto the imaging apparatus.

If the reflections that are selected do not include the unscattered beam (which will appear up at the focal point of the lens), then the image will appear dark wherever no sample scattering to the selected peak is present, as such a region without a specimen will appear dark. This is known as a dark-field image.

Electron energy loss: Different elements in a sample result in different electron energies in the beam after the sample. This normally results in chromatic aberration – however this effect can, for example, be used to generate an image which provides information on elemental composition, based upon the atomic transition during electron-electron interaction.

Phase contrast: Crystal structure can also be investigated by High Resolution Transmission Electron Microscopy (HRTEM), also known as phase contrast. When utilizing a Field emission source, of uniform thickness, the images are formed due to differences in phase of electron waves, which is caused by specimen interaction. Image formation is given by the complex modulus of the incoming electron beams. As such, the image is not only dependent on the number of electrons hitting the screen, making direct interpretation of phase contrast images more complex.

Diffraction: By adjusting the magnetic lenses such that the back focal plane of the lens rather than the imaging plane is placed on the imaging apparatus a diffraction pattern can be generated. For the single crystal case the diffraction pattern is dependent upon the orientation of the specimen and the structure of the sample illuminated by the electron beam. This image provides the investigator with information about the space group symmetries in the crystal and the crystal's orientation to the beam path.

Three dimensional imaging: As TEM specimen holders typically allow for the rotation of a sample by a desired angle, multiple views of the same specimen can be obtained by rotating the angle of the sample along an axis perpendicular to the beam. By taking multiple images of a single TEM sample at differing angles, typically in 1° increments, a set of images known as a "tilt series" can be collected. Under purely absorption contrast conditions, this set of images can be used to construct a three-dimensional representation of the sample.

1.11.2 X-ray diffraction or crystallography:

X-ray crystallography is a method of determining the arrangement of atoms within a crystal, in which a beam of X-rays strikes a crystal and diffracts into many specific directions [1]. From the angles and intensities of these diffracted beams, a crystallographer can produce a three-dimensional picture of the density of electrons within the crystal. From this electron density, the

mean positions of the atoms in the crystal can be determined, as well as their chemical bonds, their disorder and various other information.

Basic principle:

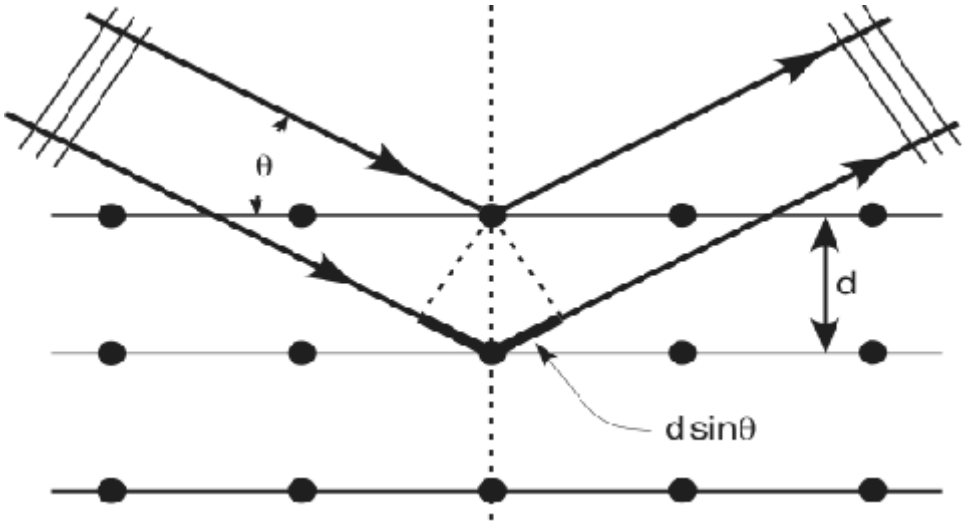

Fig. 1.8 A dramatical view of X-ray crystallography

Max Von Laue, in 1912, discovered that crystalline substances act as three-dimensional diffraction gratings for X-ray wavelengths similar to the spacing of planes in a crystal lattice. Crystals are regular arrays of atoms as shown in fig. 1.8, and X-rays can be considered waves of electromagnetic radiation. Atoms scatter X-ray waves, primarily through the atoms' electrons. Just as an ocean wave striking a lighthouse produces secondary circular waves emanating from the lighthouse, so an X-ray striking an electron produces secondary spherical waves emanating from the electron. This phenomenon is known as elastic scattering, and the electron (or lighthouse) is known as the scatterer. A regular array of scatterers produces a regular array of spherical waves. Although these waves cancel one another out in most directions through destructive interference, they add constructively in a few specific directions, determined by Bragg's law:

$$2d\sin\theta = n\lambda$$

Here d is the spacing between diffracting planes, θ is the incident angle, n is any integer, and λ is the wavelength of the beam. These specific directions appear as spots on the diffraction pattern called reflections. Thus, X-ray diffraction results from an electromagnetic wave (the X-ray) impinging on a regular array of scatterers. By varying the angle theta, the Bragg's Law conditions are satisfied by different d-spacings in polycrystalline materials. X-rays are used to

produce the diffraction pattern because their wavelength λ is typically the same order of magnitude (1-100 Angstroms) as the spacing d between planes in the crystal. In principle, any wave impinging on a regular array of scatterers produces diffraction [17]. To produce significant diffraction, the spacing between the scatterers and the wavelength of the impinging wave should be similar in size. However, visible light has too long a wavelength (typically, 5500 Angstroms) to observe diffraction from crystals. Prior to the first X-ray diffraction experiments, the spacings between lattice planes in a crystal were not known with certainty.

1.11.3 UV-visible spectroscopy:

Ultraviolet and visible spectroscopy (UV-Vis) is a reliable and accurate analytical laboratory assessment procedure that allows for the analysis of a substance [18]. Specifically, ultraviolet and visible spectroscopy measures the absorption, transmission and emission of ultraviolet and visible light wavelengths by matter. When sample molecules are exposed to light having an energy that matches a possible electronic transition within the molecule, some of the light energy will be absorbed as the electron is promoted to a higher energy orbital. An optical spectrometer records the wavelengths at which absorption occurs, together with the degree of absorption at each wavelength.

Principle: "Beer-Lambert's Law"

The change in intensity of light (dI) after passing through a sample should be proportional to the following:

(a) Path length, b , the longer the path, more photons should be absorbed

(b) Concentration, c, of sample, more molecules absorbing means more photons absorbed

(c) Intensity of the incident light (I), more photons mean more opportunity for a molecule to see a photon

Thus, dI is proportional to bcI or

$$dI/I = -kbc$$

Where k is proportionality constant, the negative sign is shown because this is a decrease in intensity of the light, this makes b, c and I always positive.

Integration of the above equation leads to Beer-Lambert's Law:

$$-\ln I / Io = kbc$$
$$-\log I / Io = 2.303kbc$$
$$\varepsilon = 2.303k$$
$$A = -\log I / Io$$
$$A = \varepsilon bc$$

A is defined as absorbance and it is found to be directly proportional to the path length, b, and the concentration of the sample, c.

Instrumentation and working: In fig. 1.9, a beam of light from a visible and/or UV light source (colored red) is separated into its component wavelengths by a prism or diffraction grating. Each monochromatic (single wavelength) beam in turn is split into two equal intensity beams by a half-mirrored device. One beam, the sample beam (colored magenta), passes through a small transparent Container containing a solution of the compound being studied in a transparent solvent. The other beam, the reference (colored blue), passes through an identical cuvette containing only the solvent. The intensities of these light beams are then measured by electronic detectors and compared. The intensity of the reference beam, which should have suffered little or no light absorption, is defined as I_0. The intensity of the sample beam is defined as I. At the wavelength where the sample absorbs a large amount of light, the detector receives a very weak sample beam. Once intensity data has been collected by the spectrometer, it is sent to the computer as a ratio of reference beam and sample beam intensities. The computer determines at what wavelength the sample absorbed a large amount of ultraviolet light by scanning for the largest gap between the two beams. When a large gap between intensities is found, where the sample beam intensity is significantly weaker than the reference beam, the computer plots this wavelength as having the highest ultraviolet light absorbance when it prepares the ultraviolet absorbance spectrum. Over a short period of time, the spectrometer automatically scans all the component wavelengths in the manner described. The ultraviolet (UV) region scanned is normally from 200 to 400 nm, and the visible portion is from 400 to 800 nm. The detector records the ratio between reference and sample beam intensities (Io/I). The ratio I / I_o are called the transmittance, and are usually expressed as a percentage (%T). The absorbance, A, is based on the transmittance:

$$A = -\log (\%T)$$

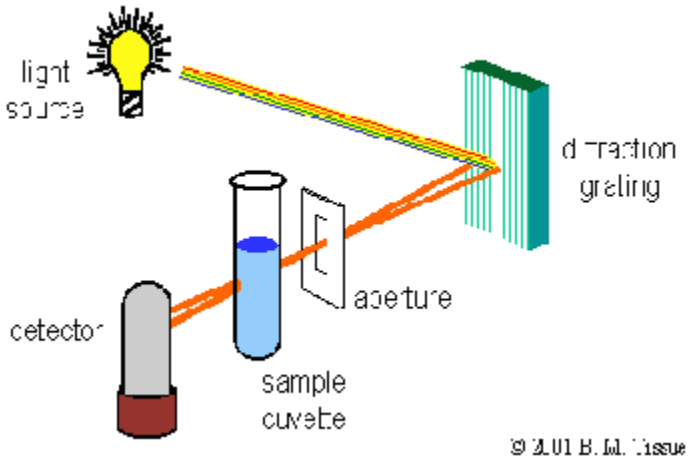

Fig. 1.9 Experimental set-up for UV Visible

1.11.4 Photoluminescence:

Photoluminescence is the light beam emitted by semiconductors mainly when electrons and holes recombine [19]. The photons that come out are very characteristic of the material. And photoluminescence spectroscopy is a contactless, nondestructive method of probing the electronic structure of materials. Light is directed onto a sample, where it is absorbed and imparts excess energy into the material in a process called photo-excitation. One way this excess energy can be dissipated by the sample is through the emission of light, or luminescence. In the case of photo-excitation, this luminescence is called photoluminescence. The intensity and spectral content of this photoluminescence is a direct measure of various important material properties. In the above fig. 1.10, Eg is the band gap energy. On the left a high energy laser photon dislodges an electron from its orbit. The electron loses energy until it reaches the bottom of the conduction band. The right hand diagram shows two possible transitions. On the left the electron combines immediately with a hole in the valence band emitting a photon of energy Eg. On the right it gets stuck in a 'mid-gap' state emitting a lower energy photon. Photo-excitation causes electrons within the material to move into permissible excited states. When these electrons return to their equilibrium states, the excess energy is released and may include the emission of light (a radiative process) or may not (a nonradiative process).The energy of the emitted light (photoluminescence) relates to the difference in energy levels between the two

electron states involved in the transition between the excited state and the equilibrium state. The quantity of the emitted light is related to the relative contribution of the radiative process.

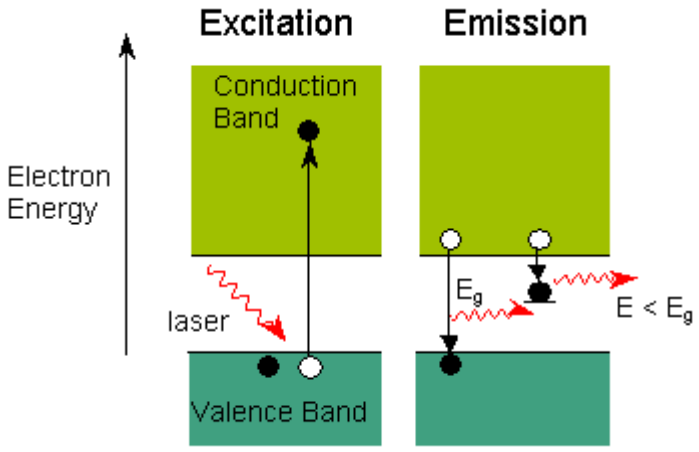

Fig. 1.10 Demonstration of PL

Photoluminescence is of two types:

Phosphorescence: Phosphorescence is a process in which energy absorbed by a substance is released relatively slowly in the form of light. Phosphorescence is a specific type of photoluminescence related to fluorescence. Unlike fluorescence, a phosphorescent material does not immediately re-emit the radiation it absorbs. The slower time scales of the re-emission are associated with "forbidden" energy state transitions in quantum mechanics. As these transitions occur less often in certain materials, absorbed radiation may be re-emitted at a lower intensity for up to several hours. The complete process of phosphorescence and fluorescence is shown on the next page in fig. 1.11

Fluorescence: Fluorescence is a luminescence that is mostly found as an optical phenomenon in cold bodies, in which the molecular absorption of a photon triggers the emission of with a longer (less energetic) wavelength. The energy difference between the absorbed and emitted photons ends up as molecular rotations, vibrations or heat. Sometimes the absorbed photon is in the ultraviolet range, and the emitted light is in the visible range, but this depends on the absorbance curve and Stokes shift of the particular fluorophore.

Photoluminescence gives information about: band gap determination, impurity levels and defect detection, recombination mechanisms and material quality.

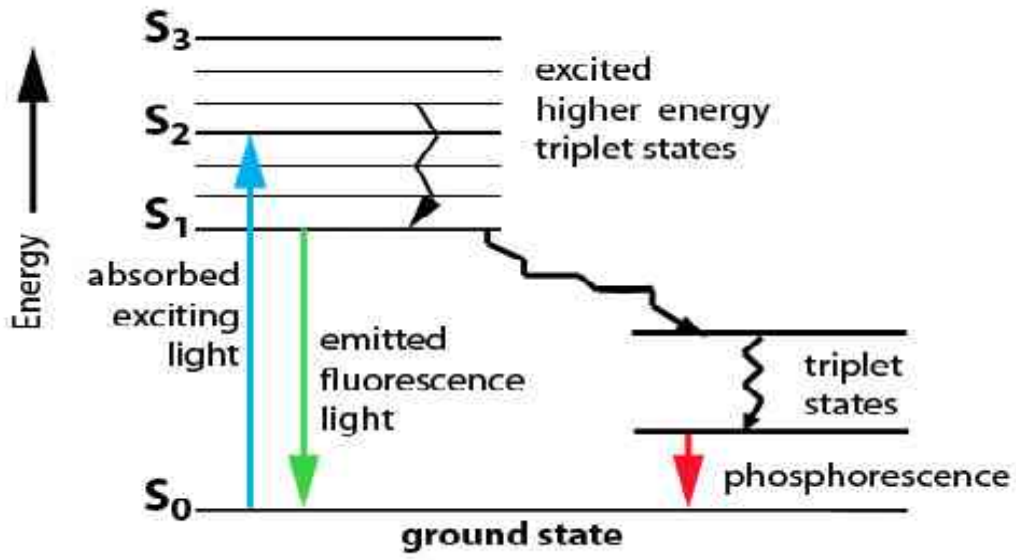

Fig. 1.11 Mechanism of phosphorescence

1.11.5 Fourier Transform Infra-Red Spectroscopy (FTIR):

Infrared (IR) spectroscopy is a chemical analytical technique, which measures the infrared intensity versus wavelength (wave number) of light. Based upon the wave number, infrared light can be categorized as far infrared (4 ~ 400cm-1), mid infrared (400 ~ 4,000cm-1) and near infrared (4,000 ~ 14,000cm-1). Infrared spectroscopy detects the vibration characteristics of chemical functional groups in a sample. When an infrared light interacts with the matter, chemical bonds will stretch, contract and bend. As a result, a chemical functional group tends to adsorb infrared radiation in a specific wave number range regardless of the structure of the rest of the molecule.

For example, the C=O stretch of a carbonyl group (shown in above fig. 1.12) appears at around 1700cm-1 in a variety of molecules. Hence, the correlation of the band wave number position with the chemical structure is used to identify a functional group in a sample. The wave ember positions where functional groups adsorb are consistent, despite the effect of temperature, pressure, sampling, or change in the molecule structure in other parts of the molecules. Thus the presence of specific functional groups can be monitored by these types of infrared bands, which are called group wave numbers.

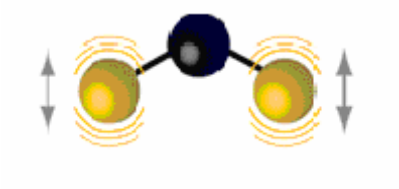

Bending mode

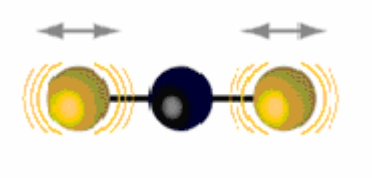

Symmetric stretching mode

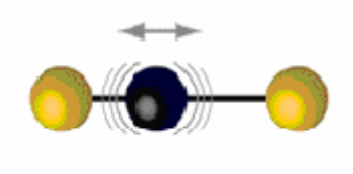

Antisymmetric stretching mode

Fig. 1.12 Representation of vibrational modes

A Fourier Transform Infrared (FTIR) spectrometer obtains infrared spectra by first collecting an interferogram of a sample signal with an interferometer, which measures all of infrared frequencies simultaneously. An FTIR spectrometer acquires and digitizes the interferogram, performs the FT function, and outputs the spectrum.

An interferometer utilizes a beam splitter to split the incoming infrared beam into two optical beams (fig. 1.13). One beam reflects off of a flat mirror which is fixed in place. Another beam reflects off of a flat mirror which travels a very short distance (typically a few millimeters) away from the beam splitter. The two beams reflect off of their respective mirrors and are recombined when they meet together at the beam splitter. The re-combined signal results from the interfering with each other. Consequently, the resulting signal is called interferogram, which has every infrared frequency “encoded” into it.

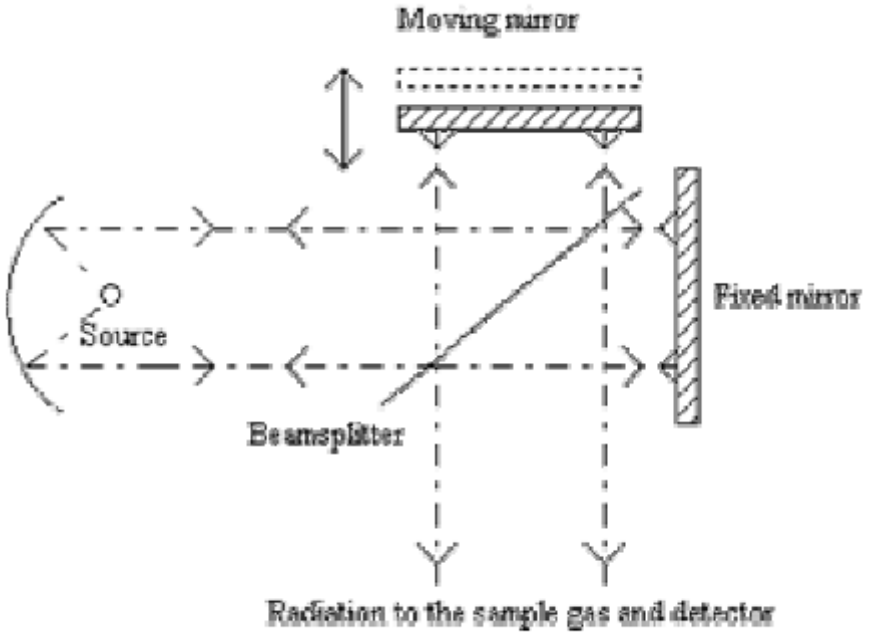

Fig. 1.13.An Interferometer

When the interferogram signal is transmitted through or reflected off of the sample surface, the specific frequencies of energy are adsorbed by the sample due to the excited vibration of function groups in molecules. The infrared signal after interaction with the sample is uniquely characteristic of the sample. The beam finally arrives at the detector and is measure by the detector. The detected interferogram cannot be directly interpreted. It has to be "decoded" with a mathematical technique in term of Fourier Transformation. The computer can perform the Fourier transformation calculation and present an infrared spectrum, which plots adsorbance (or transmittance) versus wave number.

When an interferogram is Fourier transformed, a single beam spectrum is generated. A single beam spectrum is a plot of raw detector response versus wave number. When an interferogram is measured with a sample and Fourier transformed, a sample single beam spectrum is obtained. It looks similar to the background spectrum except that the sample peaks are superimposed upon the instrumental and atmospheric contributions to the spectrum. To eliminate these contributions, the sample single beam spectrum must be normalized against the background spectrum. Consequently, a transmittance spectrum is obtained as follows:

$$\%T = I/Io$$

Where %T is transmittance; I is the intensity measured with a sample in the beam (from the sample single beam spectrum); Io is the intensity measured from the back ground spectrum. The absorbance spectrum can be calculated from the transmittance spectrum using the following equation.

$$A = -\log 10\ T, \text{ Where A is the absorbance}$$

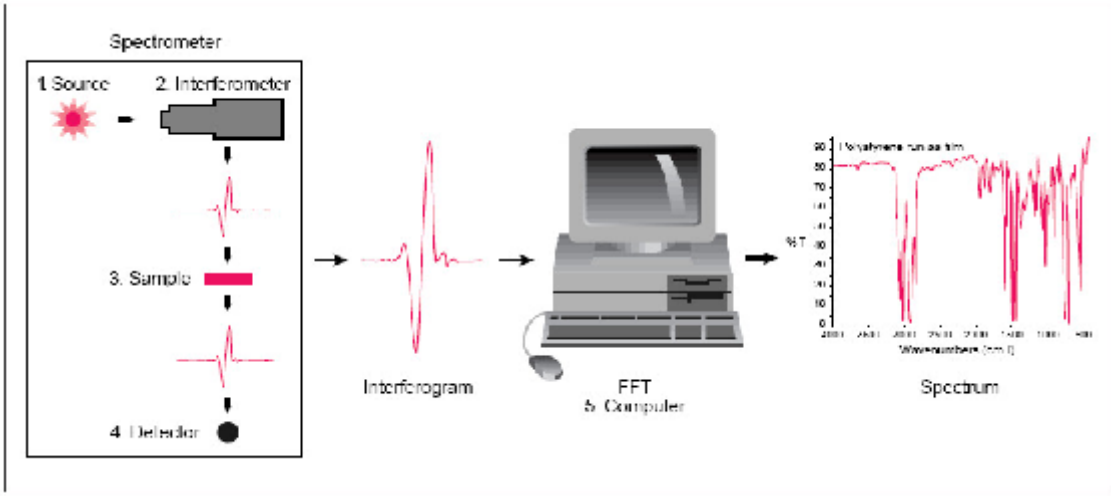

Fig. 1.14 The sample analysis process

The final transmittance/absorbance spectrum should be devoid of all instrumental and environmental contributions, and only present the features of the sample. If the concentrations of gases such as water vapor and carbon dioxide in the instrument are the same when the background and sample spectra are obtained, their contributions to the spectrum will ratio out exactly and their bands will not occur. If the concentrations of these gases are different when the background and sample spectra are obtained, their bands will appear in the sample spectrum.

Chapter – 2

Photocatalytic degradation of dye

2.1 Introduction:

Photodegradation includes photo dissociation, the breakup of molecules into smaller pieces by photons. It also includes the change of a molecule's shape to make it irreversibly altered, such as the denaturing of proteins, and the addition of other atoms or molecules [1]. A common photodegradation reaction is oxidation. This type of photodegradation is used by some drinking water and wastewater facilities to destroy pollutants.

A simple and interesting approach to extend the catalyst absorption toward visible region is the photosensitization by an appropriate dye. The dye can absorb the visible light to reach an excited state. The dye in the excite state has in general lower redox potential than the corresponding ground state. If the redox potential is lower than the conduction band of photocatalyst being used, an electron may be injected from the excited state into the conduction band, and consequently the cationic radicals and conduction band electron are formed. This process has been intensively investigated in photoelectrochemical cells (the Gratzel cell) in the absence of molecular dioxygen. However, in the presence of dioxygen, the dye itself can undergo an effective degradation. Such degradation would be desired if the dye is a target organic pollutant.

2.2 Photocatalysis:

It is the acceleration of a photoreaction in the presence of a catalyst. In catalyzed photolysis, light is absorbed by the substrate. In photogenerated catalysis the photocatalytic activity (PCA) depends on the ability of the catalyst to create electron–hole pairs, which generate free radicals (hydroxyl radicals: ·OH) able to undergo secondary reactions [20].

Photocatalysis is a fantastic way to clean facilities, houses, and living environments. By modifying and further developing this technology, we can reduce pollution in our air and water. We can even reduce the spread of infections and diseases such as SARS in hospitals. This cleaner way of life would benefit everyone around the world.

The word photocatalysis is composed of two parts:

- The prefix photo, defined as "light", [20]
- Catalysis is the process where a substance participates in modifying the rate of a chemical transformation of the reactants without being altered in the end. This substance is known as the catalyst which increases the rate of a reaction by reducing the activation energy. Hence, photocatalysis is a reaction which uses light to activate a substance which modifies the rate of a chemical reaction without being involved itself.

Photocatalysis a preferred and more advanced technique than conventional organic synthesis due to following reasons:-

- In photocatalytic reactions, both oxidation and reduction occurs simultaneously on the photocatalyst particles but in conventional reactions we need different oxidizing agent and reducing agent.
- Also in photochemical reactions there is not much need of solvents which are expensive and are difficult to dispose off. We generally use water but in conventional reactions many solvents are used.
- Photochemical reaction is a single step reaction, we can get our product just by mixing the reactant and irradiating them but conventional reactions are multi-step reactions.
- Photocatalytic reactions occur at ambient temperature and pressure so need not to maintain drastic conditions as required in conventional reactions.

2.3 Photocatalysts:

Environmental contamination, which is growing around the world or in our daily home life, is a serious social problem not to be neglected [21]. Water pollution caused by industrial and household wastes and respiratory diseases caused by air pollutants such as SOx or NOx are best examples of such contamination.

The fact that using energy to eliminate such environmental contamination increases emission of CO_2 resulting in more global warming, however, leads us to a dilemma not to use energy to achieve our anti-pollution goal.

Under such circumstances, we have come to the conclusion that we need a new material that can gently harmonize the contaminated environment to restore original conditions by using natural energy which is a part of the environment and low-cost energy supplied to our daily home life. One solution to that problem is our proposal, Photo-catalyst.

Definition and activity: Photo-catalyst produces surface oxidation to eliminate harmful substances such as organic compounds or nearby bacteria, when it is exposed to the sun or fluorescent lamp.

By applying this principle to water treatment, dissolving NOx in the air, or room air purification, photo-catalyst can be used for various steps in purifying a contaminated environment.

The function of the photo-catalyst can be divided into five major categories as follows:

- Purifying water
- Preventing contamination
- Anti-bacteria
- Deodorizing
- Purifying the air (dissolving NOx)

It might be well understood that the functions listed above are those which amplify or accelerate the functions of the sun, or ultra-violet radiation. In this sense, it is not strange to regard zinc oxide as a photo-catalyst from the viewpoint that it works as the catalyst in accelerating the functions of the light.

Photocatalyst has the following advantages over any current air purification technologies:

- Real destruction of pollutant rather than a simple transfer on a substrate
- Degradation of pollutant at ambient temperature and pressure
- Build with easily available materials and by mean of well-known techniques
- Economical, cheap and low energy consumption
- Adapted for a large range of pollutant (VOC, bacteria, mold)

Chapter - 3

Material and its photocatalytic activity

3.1 Zinc oxide:

Zinc oxide is an inorganic compound with the formula ZnO. It usually appears as a white powder, nearly insoluble in water. The powder is widely used as an additive into numerous materials and products including plastics, ceramics, glass, cement, rubber (e.g. car tyres), lubricants, paints, ointments, adhesives, sealants, pigments, foods (source of Zn nutrient), batteries, ferrites, fire retardants, first aid tapes, etc. ZnO is present in the Earth crust as a mineral zincite; however, most ZnO used commercially is produced synthetically [1].

In materials science, ZnO is often called a II-VI semiconductor because zinc and oxygen belong to the 2nd and 6th groups of the periodic table, respectively. This semiconductor has several favorable properties: good transparency, high electron mobility, wide bandgap, strong room-temperature luminescence, etc.

Chemical properties: ZnO occurs as white powder known as zinc white or as the mineral zincite. The mineral usually contains a certain amount of manganese and other elements and is of yellow to red color. Crystalline zinc oxide is thermochromic, changing from white to yellow when heated and in air reverting to white on cooling. This color change is caused by a very small loss of oxygen at high temperatures to form the non-stoichiometric $Zn_{1+x}O$, where at 800 °C, x= 0.00007. Zinc oxide is an amphoteric oxide. It is nearly insoluble in water and alcohol, but it is soluble in (degraded by) most acids, such as hydrochloric acid:

$$ZnO + 2\ HCl \rightarrow ZnCl_2 + H_2O$$

Bases also degrade the solid to give soluble zincates:

$$ZnO + 2\ NaOH + H_2O \rightarrow Na_2(Zn(OH)_4)$$

It reacts with hydrogen sulfide to give the sulfide: this reaction is used commercially in removing H_2S using ZnO powder (e.g., as deodorant).

$$ZnO + H_2S \rightarrow ZnS + H_2O$$

When ointments containing ZnO and water are melted and exposed to ultraviolet light, hydrogen peroxide is produced.

Physical properties:

Crystal structure: Zinc oxide crystallizes in three forms: hexagonal wurtzite, cubic zinc blende, and the rarely observed cubic rock salt. The wurtzite structure (shown in fig. 3.1 (a)) is most stable at ambient conditions and thus most common. The zinc blende form (shown in fig. 3.1 (b)) can be stabilized by growing ZnO on substrates with cubic lattice structure. In both cases, the zinc and oxide centers are tetrahedral. The rock salt (NaCl-type) structure is only observed at relatively high pressures about 10 GPa.

Hexagonal and zinc blende polymorphs have no inversion symmetry (reflection of a crystal relatively any given point does not transform it into itself). This and other lattice symmetry properties result in piezoelectricity of the hexagonal and zinc blende ZnO, and in pyroelectricity of hexagonal ZnO.

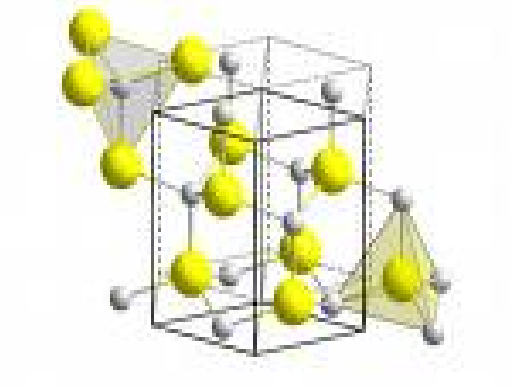

A wurtzite unit cells

Fig. 3.1 (a)

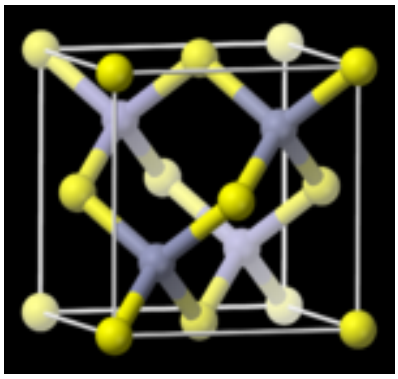

A zinc blende unit cell

Fig. 3.1 (b)

Electronic properties: ZnO has a relatively large direct band gap of ~3.3 eV at room temperature; therefore, pure ZnO is colorless and transparent. Advantages associated with a large band gap include higher breakdown voltages, ability to sustain large electric fields, lower electronic noise, and high-temperature and high-power operation. The bandgap of ZnO can further be tuned from ~3–4 eV by its alloying with magnesium oxide or cadmium oxide.

Most ZnO has *n*-type character, even in the absence of intentional doping. Nonstoichiometry is typically the origin of n-type character, but the subject remains controversial. An alternative explanation has been proposed, based on theoretical calculations, that unintentional substitutional hydrogen impurities are responsible. Controllable n-type doping is easily achieved by

substituting Zn with group-III elements such as Al, Ga, In or by substituting oxygen with group-VII elements chlorine or iodine.

Reliable p-type doping of ZnO remains difficult. This problem originates from low solubility of p-type dopants and their compensation by abundant n-type impurities. This problem is observed with GaN and ZnSe. Measurement of p-type in "intrinsically" n-type material is complicated by the inhomogeneity of samples.

Current limitations to p-doping do not limit electronic and optoelectronic applications of ZnO, which usually require junctions of n-type and p-type material. Known p-type dopants include group-I elements Li, Na, K; group-V elements N, P and As; as well as copper and silver. However, many of these form deep acceptors and do not produce significant p-type conduction at room temperature.

Electron mobility of ZnO strongly varies with temperature and has a maximum of ~2000 $cm^2/(V \cdot s)$ at ~80 K. Data on hole mobility are scarce with values in the range 5–30 $cm^2/(V \cdot s)$.

3.2 Zinc oxide at nanoscale:

Zinc oxide is an interesting compound semiconductor for ultraviolet (UV) LED and UV laser applications due to its wide direct band gap of 3.4 eV. In addition, the exciton binding energy of 60 meV exceeds the room-temperature energy of 26 meV. Therefore, ZnO can achieve excitonic UV emission, even at room temperature. ZnO nanoparticles have been investigated widely as an emission material because nanocrystallization can enhance the optical and electrical properties of wide-gap semiconductors by the quantum confinement effect. However, surface defects and impurity levels are easily generated during the nanoparticle formation process.

ZnO nanostructures can be synthesized into a variety of morphologies including nanowires, nanorods, tetrapods, nanobelts, nanoflowers, nanoparticles etc. Most nanostructures can be obtained with the vapor-liquid-solid method.

Zinc oxide is non-toxic, and compatible with skin, making it a suitable additive for textiles and surfaces that come in contact with humans. It is also used as a catalyst for methanol synthesis. The increase in surface area of nanoscale Zinc Oxide compared to larger powders has the potential to improve the efficiency of these processes. Because of such properties nanoparticles of ZnO find a lot of applications in our daily life.

3.3 How ZnO nanoparticles act as photocatalyst:

ZnO is Ⅱ-Ⅵ compound semiconductor with wide band gap (3.37 eV) and has been broadly used in photocatalysis.

Today, semiconductors are usually selected as photocatalysts, because semiconductors have a narrow gap between the valence and conduction bands. In order for photocatalysis to proceed, the semiconductors need to absorb energy equal to or more than its energy gap. This movement of electrons forms e^-/h^+ or negatively charged electron/positively charged hole pairs. The hole oxidize donar molecules [22].

Mechanism of ZnO photocatalysis:

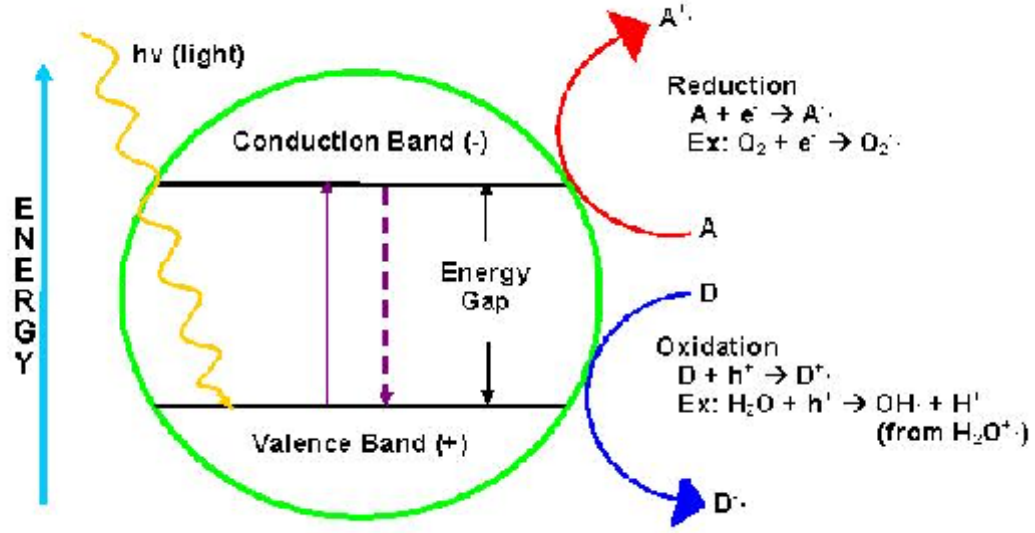

Fig. 3.2 Mechanism of photocatalytic activity of ZnO NPs

When we irradiate ZnO, the electron get excited from valence band to conduction band or can then either drop back down into the valence band resulting in recombination as heat, or it can

react with other adsorbed species. Hole will oxidize the adsorbed species, such as organic compounds, water or hydroxyl ions as shown in fig. 3.2.

$$ZnO + h\nu \rightarrow e^- + h^+$$

$$e^- + h^+ \rightarrow \text{heat}$$

$$h^+ + H^2O_{ads} \rightarrow {}^{\cdot}OH + H^+$$

$$h^+ + OH_{ads} \rightarrow {}^{\cdot}OH$$

$$h^+ + RH_{ads} \rightarrow {}^{\cdot}R + H^+$$

The electrons can also react with the compounds that are present in the solution such as oxygen and hydrogen peroxide. The electrons can be absorbed by the oxygen to form superoxide or it can react with oxygen together with hydrogen to create hydrogen peroxide. It can then react with hydrogen peroxide to create hydroxyl radicals and hydroxyl ions.

$$e^- + O_{2ads} \rightarrow O_2^-$$

$$2e^- + O_{2ads} + 2H^+ \rightarrow H_2O_2$$

$$e^- + H_2O_{2ads} \rightarrow {}^{\cdot}OH + OH^-$$

All of these produced species are highly reactive. The electrons when combined with oxygen are stopped from dropping back to the valence band and prevent the electron-hole recombination.

This means that the hole and the electron have more time to react with species adsorbed to the catalyst. A lack of dissolved oxygen would hinder the reaction as electron-hole recombination would occur far more readily, giving less time for the species to react. TiO2 is highly active

because the oxidation and reduction potential of valence band hole and conduction band electron, respectively, are appropriate for the most of the redox reactions.

3.4 Literature review:

Shriwas Ashtriputre et al. [23] synthesized ZnO nanoparticles in the quantum confinement regime. Direct band gap of 3.3eV in case of bulk ZnO should give rise to an absorption edge at ~ 375nm. However it was observed that the absorption spectra for all the samples viz. ZnO-TG1 (10^{-2} M TG), ZnO-TG2 (10^{-4} M TG) and ZnO-TG3 ($5*10^{-5}$ M TG) are not only blue-shifted with respect to 375nm absorption wavelength expected for bulk ZnO but also exhibit sharp excitonic peaks. ZnO particle size was controlled using appropriate amounts of organic capping agent viz. thioglycerol. The blue shift of all these spectra clearly indicates that particles smaller than 5.0nm have been achieved. A deliberate addition of water was made to increase the particle size. Spanhel et al have used this approach earlier. The scaling of energy gap with particle size has been explained in the effective mass approximation as well as tight binding approximation. The particle sizes calculated for the samples ZnO-TG1, ZnO-TG2 and ZnO-TG3 using effective mass approximation (EMA) are 2.6, 3.0 and 3.3nm respectively and that for ZnO-WT1 with excitonic peak at 332nm and for ZnO-WT2 with peak at 340nm are 3.6 and 4.0nm respectively. Synthesized particles are found to be stable over a long time. X-ray diffraction analysis of samples showed that the particles have a wurtzite structure. Particles of size 3.8nm can be seen in TEM analysis. The size is close to that in EMA. Diffraction pattern depicts hexagonal symmetry in agreement with XRD results. Presence of TG could be detected by performing FTIR spectroscopy. Comparison of spectrum due to thioglycerol with those of TG-capped ZnO clearly indicates the presence of thioglycerol on the nanoparticle surface.

Tahar et al. [24] reported that ZnO is used as transparent, electrically conductive films due to its low cost, higher abundance compared to other TCO materials, and stability in the presence of hydrogen plasma. The room temperature conductivity of the ZnO films can be changed by several orders of magnitude through the creation of intrinsic donors (oxygen vacancies or metal atoms on interstitial lattice sites) or by doping with Al, In, Ga, B, or group-VII elements such as fluorine. The extrinsic donors due to the dopant atoms are more stable than the intrinsic donors due to native defects especially when the films are subjected to higher temperatures.

Considerable attention has been devoted to study the effect of boron on the electrical and optical properties of zinc oxide that have been synthesized primarily by chemical vapor deposition. We are not aware of attempts to deposit the material by sol-gel technique. In this article they reported on the physical properties of BZO films prepared by dip-coating technique. The electrical and optical properties were investigated according to various deposition parameters. Boron tri-i-propoxide was added to provide a stock solution with specific molar ratio of boron to zinc. Part of the clear solution was transferred to a glass petri dish and allowed to gel at room temperature. The dried gel was transparent. Crack free and highly adherent thin films were dipcoated on glass substrates. After each deposition, samples were dried at 100^0C for 10 min for solvent removal. Densification and crystallization were accomplished by subsequently annealing the layers at 400–650^0 C for 30 min in air. Deposition and heat treatment were repeated to build thicker coatings. Selected samples were subjected to vacuum annealing (□ 10−3 Torr) at 400–450^0 C. The electrical resistivity curve with doping shows a minimum around 0.8 at. %. Excess boron caused a drop of the carrier mobility without acting as donors. Post-deposition annealing sequence was crucial for dopant partial regeneration. Films with an average optical transmittance exceeding 90% can be achieved reproducibly.

Jiaguo yu et al. [25] reported that ZnO hollow spheres with porous crystalline shells were one-pot fabricated by hydrothermal treatment of glucose/$ZnCl_2$ mixtures at 180°C for 24 h, and then calcined at different temperatures for 4 h. The as-prepared samples were characterized by X-ray diffraction, scanning electron microscopy, transmission electron microscopy and nitrogen adsorption−desorption isotherms. The photocatalytic activity of the as-prepared samples was evaluated by photocatalytic decolorization of Rhodamine B aqueous solution at ambient temperature. The results indicated that the average crystallite size, shell thickness, specific surface areas, pore structures, and photocatalytic activity of ZnO hollow spheres could be controlled by varying the molar ratio of glucose to zinc ions (R). With increasing R, the photocatalytic activity increases and reaches a maximum value at R = 15, which can be attributed to the combined effects of several factors such as specific surface area, the porous structure and the crystallite size. Further results show that hollow spheres can be more readily separated from the slurry system by filtration or sedimentation after photocatalytic reaction and reused than conventional powder photocatalyst. After many recycles for the photodegradation of RhB, the

catalyst does not exhibit any great loss in activity, confirming ZnO hollow spheres is stability and not photo corroded. The prepared ZnO hollow spheres are also of great interest in solar cell, catalysis, separation technology, biomedical engineering, and nanotechnology.

Mohammad A. Behnajady et al. [26] tested the photocatalytic activity of silver-doped ZnO by photocatalytic degradation of C.I. Acid Red 88 (AR88) as a model contaminant from monoazo textile dyes. Silver-doped ZnO was prepared by photo deposition (PD) method. Results show that silver-doped ZnO is more efficient than undoped ZnO at photocatalytic degradation of AR88. The PD method parameters such as irradiation time, calcination temperature and silver content of doping were effective on the photoactivity of silver-doped ZnO. Silver content had an optimum value of 0.5% for achieving high photocatalytic activity. In the real wastewater from a textile-dyeing factory color removal with pure and silver-doped ZnO after 18 min of irradiation were 45 and 90%, respectively.

Xue-Lian Bai et al. [27] gave the idea that the mixed oxide photocatalysts, ZnO-Zn_2SnO_4 (ZnO-ZTO) nanowires with different sizes were prepared by a simple thermal evaporation method. The ZnO-ZTO nanowires were characterized with a scanning electron microscope, X-ray diffraction, high-resolution transmission electron microscopy, energy-dispersive spectrometer, and X-ray photoelectron spectra. The photocatalytic activity of the ZnO-ZTO mixed nanowires were studied by observing the photodegradation behaviors of methyl orange aqueous solution. The results suggest that the ZnO-ZTO mixed oxide nanowires have a higher photocatalytic activity than pure ZnO and Zn_2SnO_4 nanowires. The photocatalyst concentration in the solution distinctly affects the degradation rate, and our results show that higher photodegradation efficiency can be achieved with a smaller amount of ZnO-ZTO nanowire catalyst, as compared to the pure ZnO and ZTO nanowires. Moreover, the photocatalytic activity can also be enhanced by reducing the average diameter of the nanowires. The activity of pure ZnO and ZTO nanowires are also enhanced by physically mixing them. These results can be explained by the synergism between the two semiconductors.

Jozsef Nemeth et al. [28] reported that nanocrystalline ZnO particles have been prepared with different methods using zinc cyclohexanebutyrate as precursor in dimethyl sulfoxide (DMSO)

medium via alkaline hydrolysis. A series of preparations were carried out in the presence of layered silicates (kaolinite and montmorillonite). It was revealed by different measurement techniques that the presence of the clay minerals has a stabilization influence on the size of the ZnO nanocrystals.UV-vis absorption spectra show a blue shift when the nanoparticles are prepared in the presence of the clay minerals. The average particle diameters calculated from the Brus equation ranged from 2.6 to 13.0 nm. The UV-vis spectra of the synthesized nanoparticles did not show any red shift after 2-3 days, demonstrating that stable ZnO nanocrystals are present in the dispersions. The presence of the ZnO nanoparticles was also proven by fluorescence measurements. A number of the nanoparticles are incorporated into the interlamellar space of the clays, and an intercalated structure is formed as proven by X-ray diffraction (XRD) measurements. The size of the nanoparticles in the interlamellar space is in the range of 1-2 nm according to the XRD patterns. Transmission electron microscopy and high-resolution transmission electron microscopy investigations were applied to determine directly the particle size and the size distribution of the nanoparticles.

Hiroyuki Usui et al. [29] observed that ZnO nanoparticles act as an emission material because nanocrystallization can enhance the optical and electrical properties of wide-gap semiconductors by the quantum confinement effect. However, surface defects and impurity levels are easily generated during the nanoparticle formation process. The lattice defects of ZnO, such as oxygen vacancies, are known to cause a green emission. Several surface treatment approaches, such as annealing in oxygen, surface coating by polymeric materials, embedding in a silica matrix, and face-to-face annealing, succeeded in suppressing the green emission intensity from ZnO nanostructures. However, these processes require multiple steps for obtaining high-intensity UV emission without green emission. After several investigations they observed that surfactant molecules play a crucial role in passivating defects on ZnO nanoparticle surfaces. So they prepared ZnO nanoparticles by laser ablation of a zinc metal plate in a liquid environment using different surfactant (cationic, anionic, amphoteric, and nonionic) solutions. The nanoparticles were obtained in deionized water and in all surfactant solutions except the anionic surfactant solution. The average particle size and the standard deviation of particle size decreased with increasing amphoteric and nonionic surfactant concentrations. With the increase of the amphoteric surfactant concentration, the intensity of the defect emission caused by oxygen

vacancies of ZnO rapidly decreased, while the exciton emission intensity increased. This indicates that anionic oxygen in the amphoteric surfactant molecules effectively occupied the oxygen vacancy sites at the ZnO nanoparticle surface due to charge matching with the positively charged ZnO nanoparticles.

K Byrappa et al. [30] studied the sunlight mediated photocatalytic degradation of Rhodamine B (RB) dye using hydrothermally prepared ZnO (T = 150°C and P ~ 20–30 bars). Zinc chloride was used as the starting material along with sodium hydroxide as a solvent in the hydrothermal synthesis of ZnO. Different durations were tried to obtain pure ZnO phase, which was later confirmed through powder X-ray diffraction. The photocatalytic behavior of the prepared ZnO was tested through the degradation of RB. The disappearance of organic molecules follows first-order kinetics. The effect of various parameters such as initial dye concentration, catalyst loading, pH of the medium, temperature of the dye solution, on the photo degradation of RB were investigated. The thermodynamic parameters of the photodegradation of RB, like energy of activation, enthalpy of activation, entropy of activation and free energy of activation revealed the efficiency of the process. An actual textile effluent containing RB as a major constituent along with other dyes and dyeing auxiliaries was treated using hydrothermally synthesized ZnO and the reduction in the chemical oxygen demand (COD) of the treated effluent revealed a complete destruction of the organic molecules along with colour removal.

Ji-Chuan Xu et al. [31] reported that the ZnO cannot be used as photocatalyst only in its pure form or in doped form but zinc ions also acts as surface dopant like surface dopant in TiO_2. The Zn ions surface-doped TiO_2 nanotubes were synthesized via an assembly process based on ligand exchange reaction and with additional thermal treatment. First the ligand exchange reaction between zinc acetylacetonate and hydroxide radicals on TiO_2 surface introduced the Zn ions onto the surface of TiO_2 nanotubes, then the $Zn(acac)_2$ assembled TiO_2 nanotubes were calcined at an optimal temperature (400 °C) to eliminate the organic ligands. The as-prepared Zn ions surface-doped TiO_2 nanotubes showed a further improvement on the photocatalysis activity for degradation of methyl orange in water.

S-M Zhu et al. [32] observed that the contamination of ground water systems by organic chemicals poses a serious environmental threat. ZnO have received considerable attention for their ability to remove pollutants. In the last decade, various synthetic approaches have been developed to produce ZnO. However, ZnO nanoparticles are prone to aggregation due to a large surface area and high surface energy. Thus, to solve this problem, it is necessary to modify the surface of the ZnO nanoparticles and several physical and chemical methods for modifying the surface of ZnO nanoparticles have been proposed. So S-M Zhu proposed the idea of reactive ion exchange synthesis of high purity ZnO nanoparticles. They reported that high purity ZnO nanocrystals were prepared by a one-step reactive ion exchange procedure Zn $(NO_3)_2$ and strong basic anion-exchange resins were used as the raw materials. The particle sizes of the nanocrystals were between 30 and 50 nm. The products were characterized by X-ray diffraction, scanning electron microscopy, energy dispersive X-ray spectroscopy, Fourier transform infrared spectroscopy, and ultraviolet–visible spectroscopy. The ZnO nanocrystals had a hexagonal wurtzite structure, whose ratio of length to diameter was more than 10:1. The synthesized ZnO powders were successfully used as catalyst materials for methyl orange photodegradation.

Takuyu Tsuzuki et al. [33] gave the idea of reduced photocatalytic activity of ZnO nanoparticles by doping with manganese. As the intense ultra violet radiation in Australia is causing major skin cancer problems and accelerated degradation of materials such as textiles, plastics, timbers, paints and dyes, ZnO nanoparticles are considered to be one of the most effective UV blocking agents for their broad UV absorption spectrum, low toxicity and low production/material cost. However, the inherent photo-catalytic activity of ZnO hinders the use of ZnO nanoparticles in many applications. So Takuyu Tsuzuki et al. gave the idea of reduced photocatalytic activity of ZnO nanoparticles by doping with manganese. Then ZnO nanocrystalline powders doped with up to 5 at% manganese were prepared using a sol-gel process. The powder consisted of primary particles of ~ 10 nm in diameter and had a high specific surface area. XRD study revealed that up to ~ 3 at% manganese ions were doped in the ZnO crystal lattice. The photoactivity of undoped and doped ZnO nanocrystalline powders was evaluated by monitoring the photo-bleaching of the aqueous solutions of Rhodamine B dye in the presence of ZnO under the simulated sunlight. Manganese doped zinc oxide exhibited significantly reduced photoactivity compared to undoped zinc oxide. This reduction is important for ZnO nanoparticles to be used as UV shielding agents

to protect organic substrates. Further investigation is planned for (i) the determination of the location of manganese ions, (ii) the study of the photocatalytic activity of manganese doped ZnO in the doping level lower than 1 at% and (iii) the mechanism of the reduction of photocatalysis by manganese ions on particle surfaces.

A.Dodd et al. [34] investigated the effect of doping with cobalt and manganese oxide on the photocatalytic activity of nanoparticles of zinc oxide. Zinc oxide powders with controlled particle size, minimal agglomeration, and controlled chemical composition were manufactured by mechanochemical processing. The photocatalytic activity of the powders was measured using the spin trapping technique with electron paramagnetic resonance spectroscopy. It was found that the addition of cobalt oxide decreased the yield of photogenerated hydroxyl radicals. In contrast, doping with manganese oxide was found to substantially increase the rate of radical production.

Manoj Sharma et al. [35] reported the study of energy transfer mechanism from different capping agents to intrinsic luminescent vacancy centres of zinc sulphide (ZnS). Nanoparticles of capped and uncapped ZnS are prepared by co-precipitation reaction. These nanoparticles are sterically stabilized using organic polymers—poly vinyl pyrrolidone, 2-mercaptoethanol and thioglycerol. Monodispersed nanoparticles were observed under TEM for both capped and uncapped ZnS nanopowders. However, for uncapped ZnS nanopowders, tendency for formation of nanorod like structure exists. Size of ZnS crystallites was calculated from X-ray diffraction pattern. The primary crystallite size estimated from X-ray diffraction pattern is 1.95–2.20 nm for capped nanostructures and 2.2 nm for uncapped nanostructures. Band gap measurement was done by UV–visible spectrophotometer. Excitation and emission spectra are also performed in order to compare optical properties in various samples. Increase in emission intensity and band gap has been observed by adding different capping agents in comparison to uncapped ZnS nanoparticles. The results show that in capped ZnS nanoparticles the mechanism of energy transfer from capping layer to photoluminescent vacancy centres is more pronounced.

Chapter - 4

Experimental

Zinc oxide (ZnO) nanoparticles were synthesized by chemical precipitation method [35-37] by adding appropriate amount of zinc acetate solution and OH^- as precipitating anion formed by decomposition of sodium hydroxide (NaOH). Homogeneous solutions of zinc acetate and sodium hydroxide were prepared in an aqueous media. 0.5 M zinc acetate ($Zn(CH_3COO)_2.2H_2O$) solutions in aqueous medium were added in 0.5 M sodium hydroxide solution and stirred continuously for few hours at room temperature. As a capping agent poly-vinyl pyrrolidone (PVP) (1% & 2% by wt), mercapto ethanol (ME) (1% & 2% by wt) and thioglycerol TG was also added to the reaction medium for controlling the particle size. The precipitate appears soon after the addition of capping agent indicating the flocculation phenomenon occurring in the system. The precipitated particles were filtered using whatman 40 filter paper. To remove the last traces of adhered impurities, the particles were washed several times using ethanol. The washed particles were annealed at 300^0C in vaccuum. Annealing in vacuum at 300 °C significantly reduces the carboxylate and hydroxyl impurities in the samples. The total luminescence intensity (UV Visible) increases as the particle size grows for both the unannealed and annealed samples. The ZnO nanoparticles were characterized by X-ray diffraction (XRD) using Panalytical X'Pert Pro with Cu Kα radiation. Crystallite size of ZnO nanoparticles were calculated by following Scherrer's equation,

$$D = k\lambda / \beta\cos\theta \qquad (4.1)$$

where k=0.9, D- crystallite size (Å), λ(Å) the wavelength of Cu Kα radiation and β– corrected half width of the diffraction peak. Optical absorbance of the ZnO particles were recorded with a UV-Visible spectrophotometer (Model: Hitachi - 2800) with a scan speed of 200 nm/min in the range 190–600 nm. For the measurement of UV-visible absorbance the dried particles were dispersed in ethanol by sonication process.

Chapter - 5

Results and Discussion

5.1 XRD analysis:

The representative XRD pattern of as-prepared capped and uncapped ZnO nanoparticles is shown in Fig. 5.1a, Fig. 5.1b and Fig. 5.1c. Fig. 5.1d shows XRD pattern of intermediate compound of zinc acetate and sodium hydroxide which is not matching with any of possible ZnO structures according to JCPDS files. So after annealing this synthesized mixture for 3 hours at 300°C these powders were further characterized for structural studies using XRD. All diffraction peaks can be readily indexed. Peaks marked match well with the hexagonal wurtzite structure (space group P63mc) of ZnO with estimated lattice constants a=3.2498 and c=5.2066 Å much comparable with the given values in JCPDS (80-0075). No characteristic peak was observed for other impurities, such as Zn $(OH)_2$. Furthermore, all diffraction peak positions of ZnO in capped and uncapped NPs accord with that of pure ZnO. The peak broadening in the XRD pattern clearly indicates that very small nanocrystals are present in the samples. The diameter (D) of ZnO QDs can be calculated by using Debye-Scherrer formula

$$D = 0.9\lambda/B\cos\theta_B \qquad (1)$$

where λ is the X-ray wavelength (0.15418 nm), θ_B is the Bragg diffraction angle, and B is the full width at half-maximum. According to the diffraction peak positions and the width at half-maximum, the mean size of ZnO QDs can be estimated to be approximately 12nm to 15 nm for TG capped ZnO NPs and for ME capped ZnO size lies b/w 42nm to 45nm. For uncapped ZnO NPs the average size is 26nm.

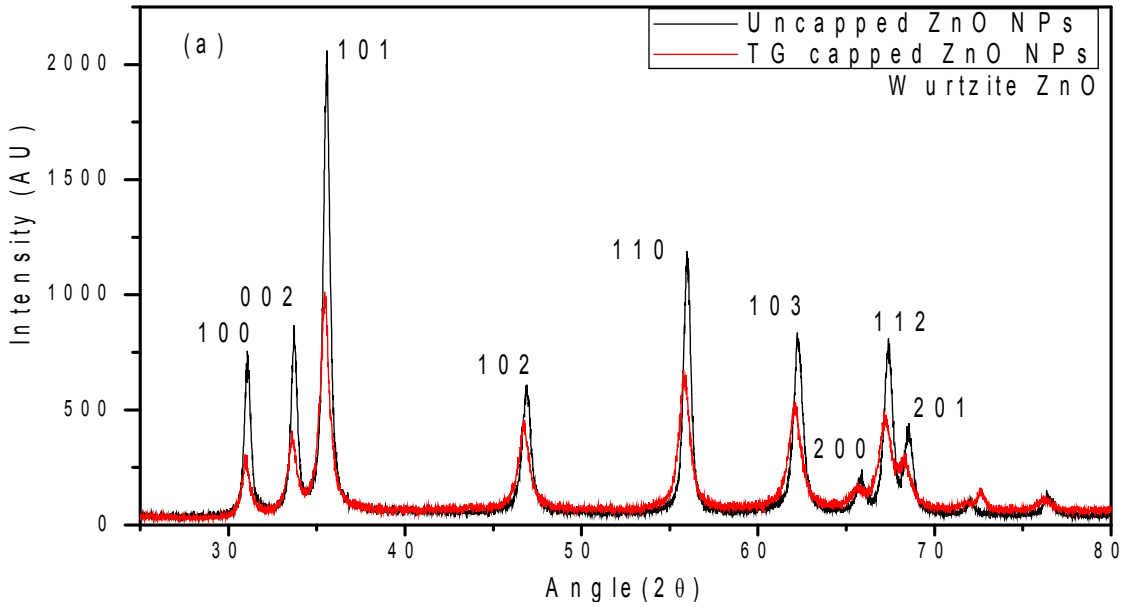

Fig.5.1 (a) XRD pattern of as-prepared capped and uncapped ZnO nanoparticles

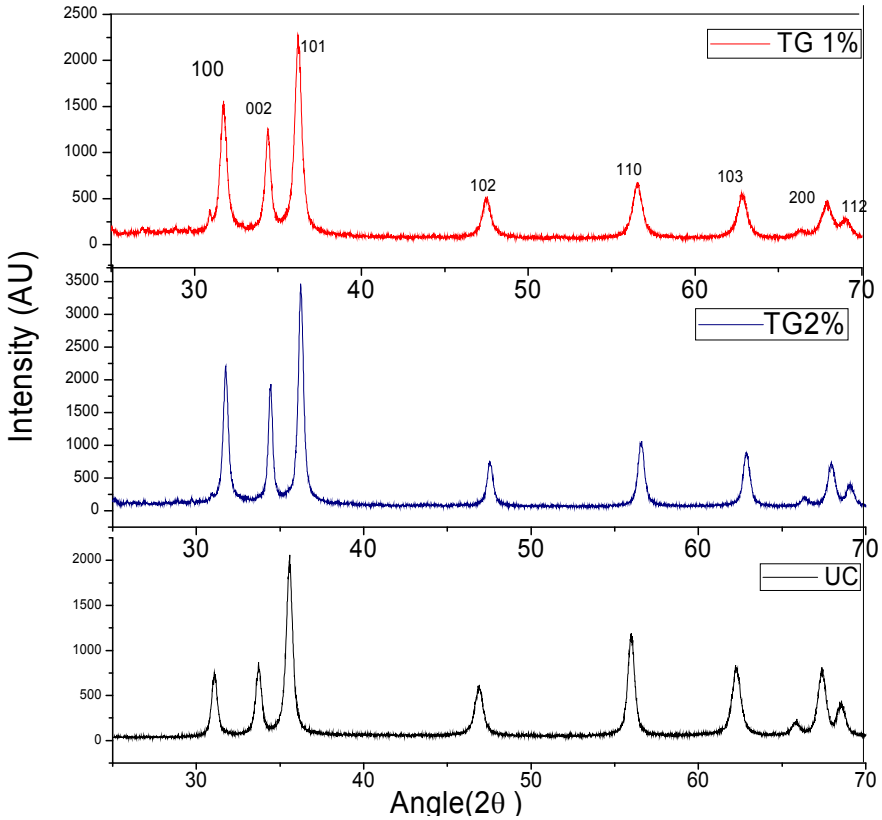

Fig.5.1 (b) XRD pattern of as-prepared capped and uncapped ZnO nanoparticle

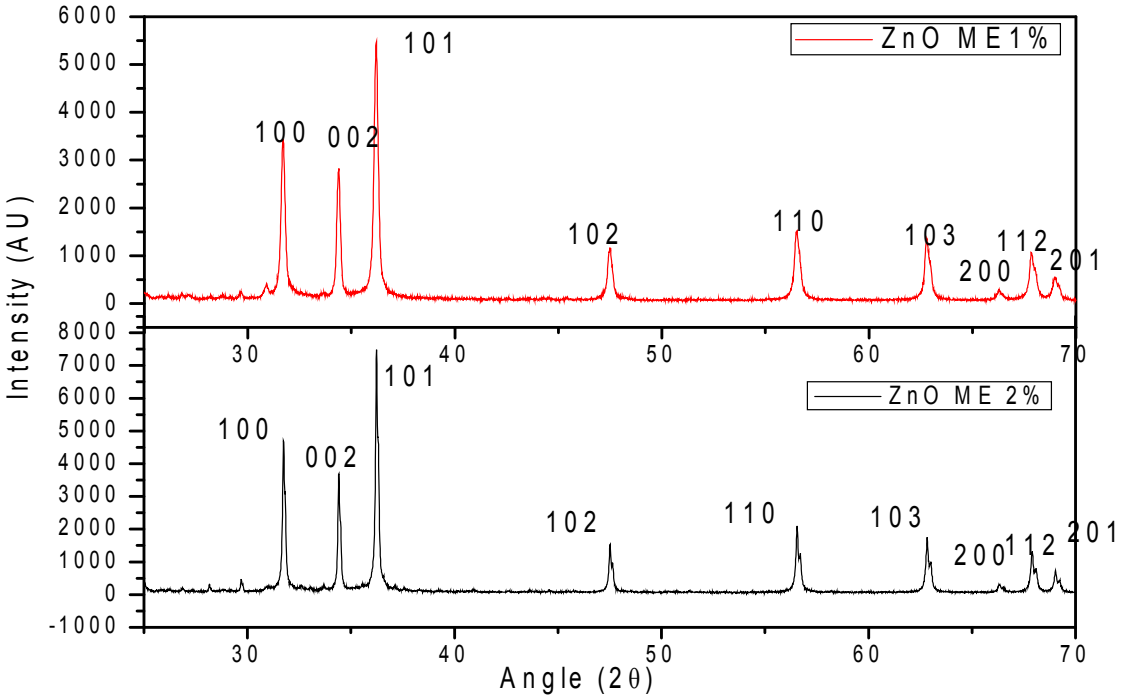

Fig. 5.1 (c) showing the XRD pattern of ME capped ZnO nanoparticles

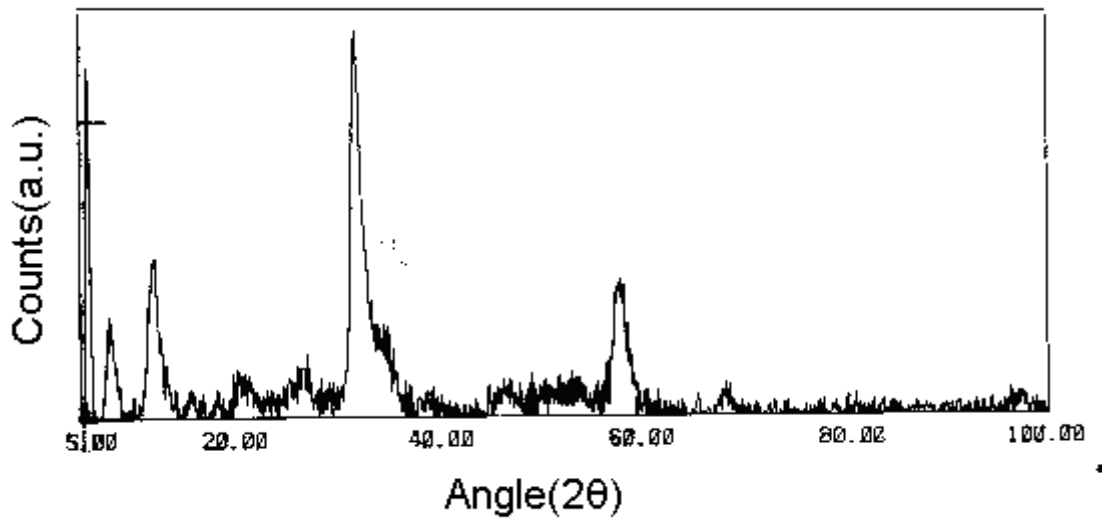

Fig.5.1 (d) XRD pattern of as-prepared intermediate nanoparticles using precursors zinc acetate and sodium hydroxide**.**

5.2 UV Visible analysis:

The optical transmission spectra of the $Zn(OH)_2$, TG capped, uncapped ZnO nanoparticle, ME capped (1% & 2% by weight) was recorded as a function of wavelength in the wavelength range 200–900 nm as shown in figure 5.2(a, b, c, d). The calculated bandgap was found to be in the range of 3.31 to 3·42 eV of the ZnO nanopowder which is shown below in the Table I corresponding to the used capping agents and is found greater than the reported bandgap value of ZnO bulk i.e. Eg = 3·30eV (Zu et al. 1997). The difference in the bandgap values ranging from 3·1– 3·3 eV is one of the curious features of the literature on ZnO. Srikant and Clarke (1998) investigated the optical bandgap of ZnO single crystals at room temperature using a variety of optical techniques (i.e. conventional reflection and transmission absorption mea measurement, spectroscopic ellipsometry, Fourier transform infared spectroscopy and photoluminescence) and reported three different Eg which is greater than the bandgap in the case of bulk values of 3·1, 3·2 and 3·3 eV. They concluded that the room temperature bandgap of ZnO was 3·3 eV, whereas reports of an apparent bandgap at 3·1 and 3·2 eV were due to the existence of a valence band–donor transition at 3·15 eV which can dominate the absorption spectrum when the bulk, as distinct from the surface, of a single crystal is probed.

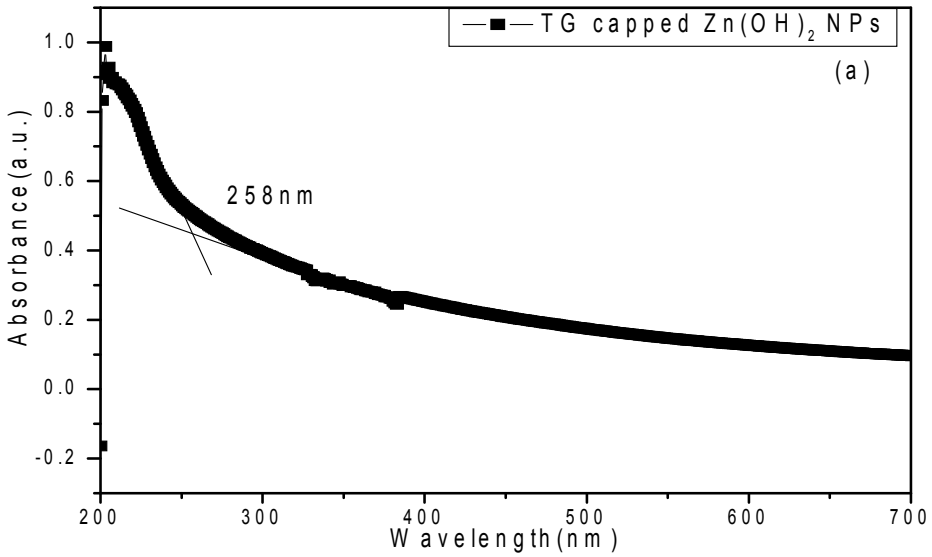

Fig 5.2 (a) UV- Visible absorption spectra of TG capped Zn $(OH)_2$ complex

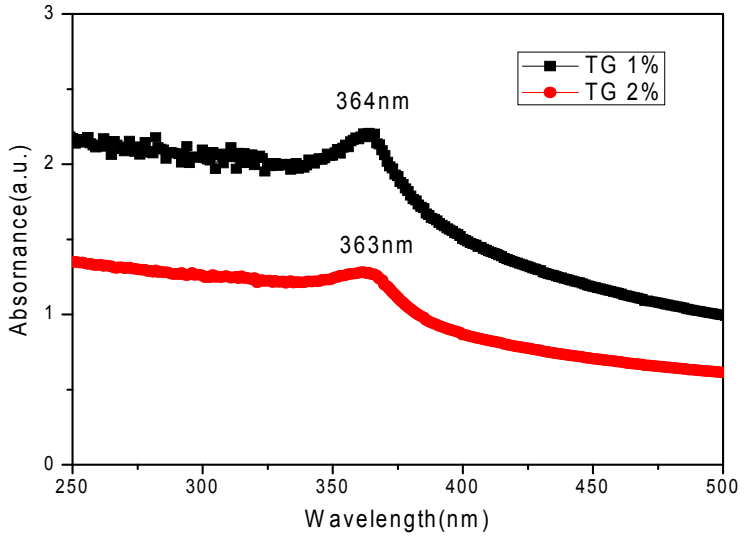

Fig. 5.2 (b) UV Visible absorption spectra of TG capped and uncapped ZnO NPs

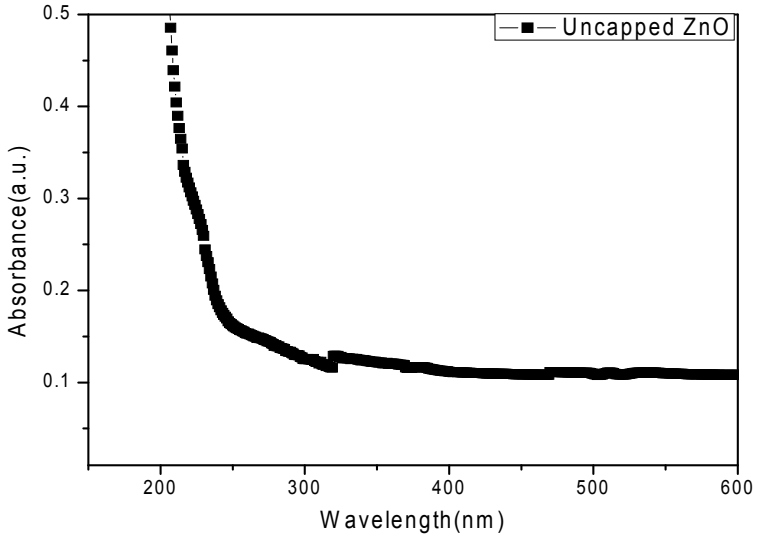

Fig. 5.2 (c) UV Visible absorption spectra for uncapped ZnO NPs

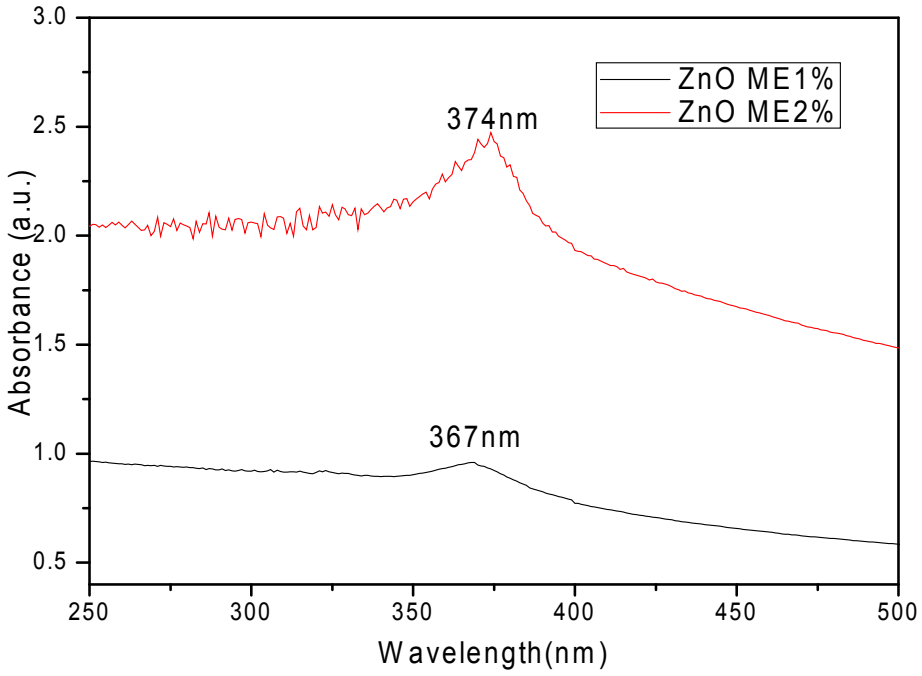

Fig 5.2 (d) UV Visible absorption spectra for ME capped ZnO NPs

Table I: Band gaps corresponding to the different capping agents

Capping agent	%age by weight	Absorption wavelength (nm)	Band gap (eV)
TG	1%	364	3.41
TG	2%	363	3.42
ME	1%	374	3.32
ME	2%	367	3.38

5.3 SEM and EDX analysis:

From Fig. 5.1(a), it is also clear that ZnO nanoparticles exhibit significant confinement effects for a particle diameter less than ~26 nm. Scanning electron microscope (SEM) micrograph is shown in Fig. 5.3(a), which demonstrates clearly the formation of ZnO nanoparticles. The

corresponding EDX spectrum is shown in Fig. 5.3(b) which shows presence of zinc and oxygen ions in larger amounts along with some carbon and nitrogen in less amount which can be assigned to surface adsorbed polymer thioglycerol. Table II shows atomic and weight % of all constituents present in sample.

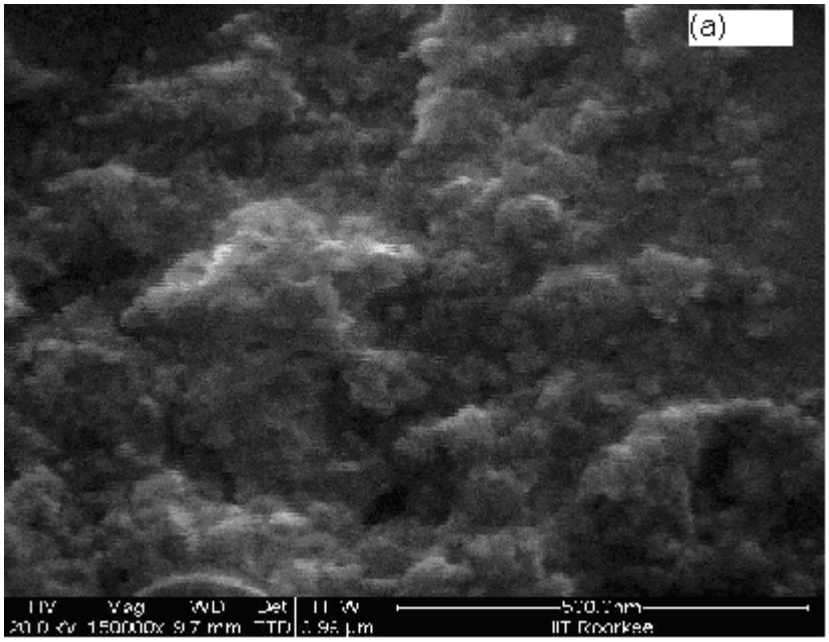

Fig 5.3 (a) Scanning electron microscopy analysis of TG capped ZnO NPs

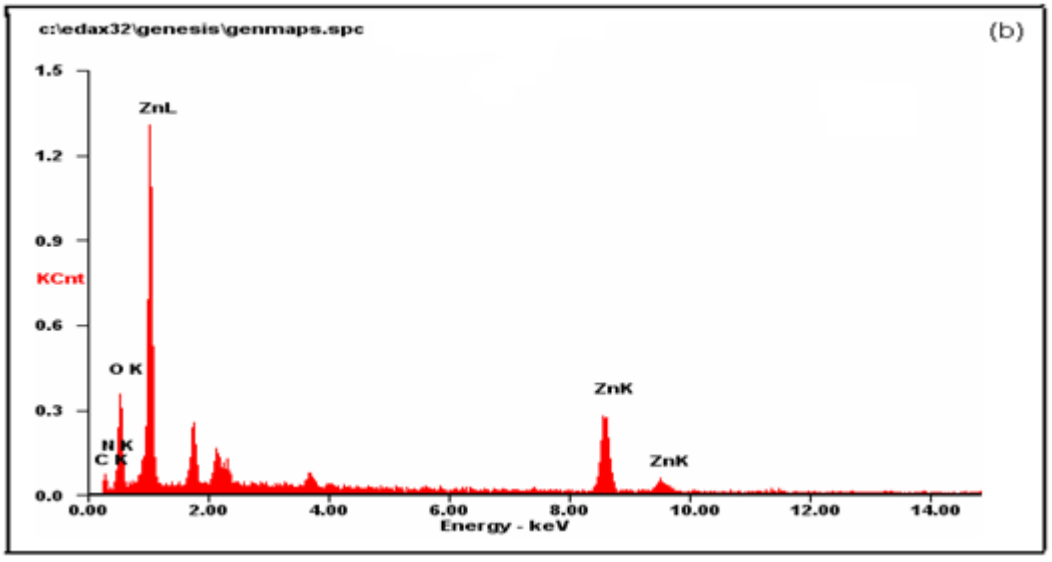

Fig. 5.3 (b) EDX analysis of TG capped ZnO NPs

Table II - EDX analysis of TG capped ZnO NPs

Element	Wt. %	At. %
CK	13.03	29.90
NK	01.02	02.01
OK	24.45	42.14
ZnK	61.50	25.94
Matrix	Correction	ZAF

5.4 Photoluminescence:

Fig 5.4 (a) shows excitation spectra of synthesized TG capped and uncapped ZnO NPs. Both samples shows excitonic peak near 345nm which is blue shifted than bulk ZnO which comes at 380nm. Fig. 5.4 (b) shows the photoluminescence (PL) emission from Zn $(OH)_2$ complex, TG capped and uncapped ZnO nanoparticles dispersed in double distilled water. We have collected PL spectra for excitation wavelengths 320 nm. As demonstrated in Fig. 5.4 (b) that PL emission intensity of TG capped particles is increased by ~ 2.5 times under 320 nm excitation in comparison to uncapped ZnO NPs. A strong maximum at 460 nm and at 419 nm wavelength appeared in the PL spectrum of $Zn(OH)_2$ complex, under the excitation at 320 nm in both the samples. However, the whole PL emission spectrum covers the 400-550 nm of the visible region of the electromagnetic spectrum. The broad visible photoluminescence band as shown in Fig5.4 (b) has actually been reported earlier in bulk ZnO as well as in ZnO quantum dots. It is also shown that TG ZnO NPs shows high emission intensity and considerable blue shift in comparison to uncapped ZnO NPs. In Fig 5.4 (b) it is shown that PL intensity blue shifts from 419-450nm to 363nm in TG capped ZnO NPs.

It has been shown in that the visible emission from nanocrystalline ZnO particles is due to a transition of a photo-generated electron from the conduction band to a deeply trapped hole. In ZnO nanoparticles along-with the visible green emission, UV excitonic emission is also reported. Therefore, for efficient visible emission a step must be involved in which the photo-generated hole is trapped efficiently somewhere in the particle. The rate of this hole trapping must be much faster than the radiative recombination rate of the exciton emission. Because of the large surface-

to-volume ratio of our ZnO particles, efficient and fast trapping of photo-generated holes at surface sites can be expected. A probable candidate for the trapping of holes is O_2 ions at the surface. Trapping of a photo-generated hole at the surface is also in agreement with the size-dependence of the emission intensities. The rate for a surface trapping process increases as the particle size decreases since the surface-to-volume ratio increases and thus the blue- green emission is observed in our sample with reduced particle size of 26 nm.

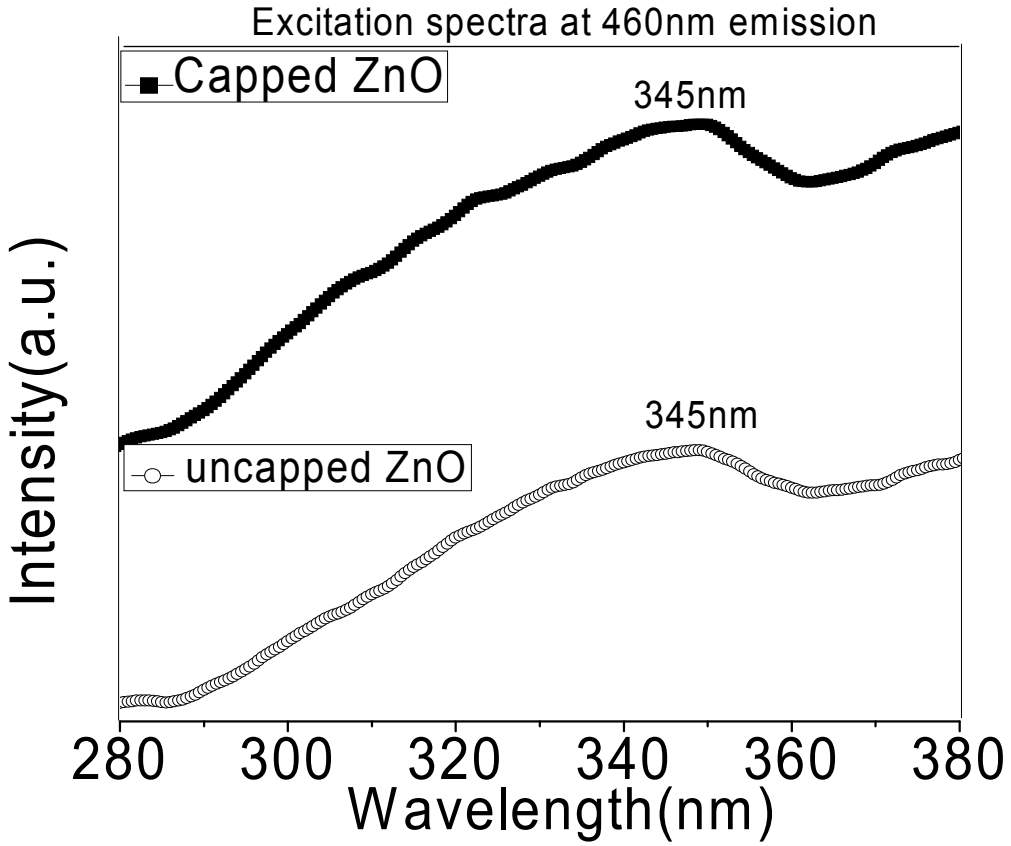

Fig 5.4 (a) Excitation spectra of synthesized capped and uncapped ZnO NPs

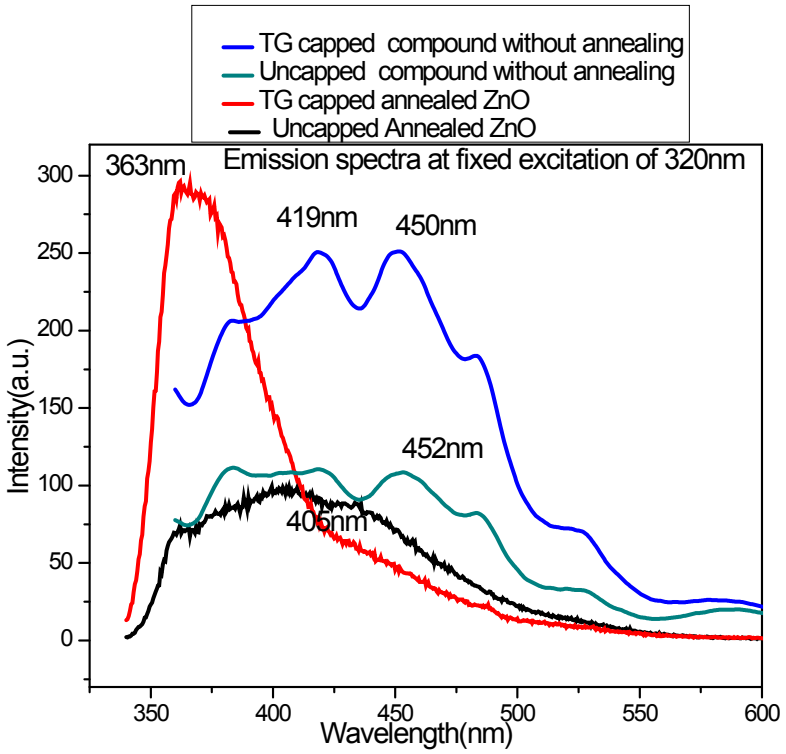

Fig 5.4 (b) Emission spectra of capped and uncapped ZnO NPs at fixed excitation wavelength of 320nm.

Table III: Excitation and emission spectra of ZnO NPs in PL

Compound	Excitation spectra	Emission spectra
TG capped ZnO w/o annealing	320nm	419nm,450nm
TG capped annealed ZnO	320nm	363nm
Uncapped ZnO w/o annealing	320nm	452nm
Uncapped annealed ZnO	320nm	405nm

5.5 Photocatalytic degradation of dye (crystal violet):

Degradation of dye crystal violet was done using TG 2% capped ZnO NPs. The absorption spectera is shown below in the fig. 6. First of all 50ppm of crystal violet dye was taken and in the absence of NPs it showed absorption peak at 550nm. After that the ZnO NPs were added to the

dye and the solution was kept in UV reactor to record the data after a particular time interval. UV light is being absorbed by the NPs since their absorbance lies in this range as shown above in UV Visible analysis. So ZnO NPs transfer energy to dye molecules which further degrade it. The spectra showed that on the addition of NPs the absorbance of dye decreased as the time passed. The UV Visible spectra were observed after every 20 minutes and the absorbance was different in all the spectra. It was maximum at minimum time. The spectra were observed till the dye showed minimum absorbance along with the complete color removal. This minimum absorbance and the color removal occurred in 2 hours and 20 minutes and this results into the complete degradation of dye. As the Fig. 6 shows the red peak is at zero time having the maximum absorbance and as the absorbance decreases the peaks are lowered and different colored peaks show different absorbance at different time interval.

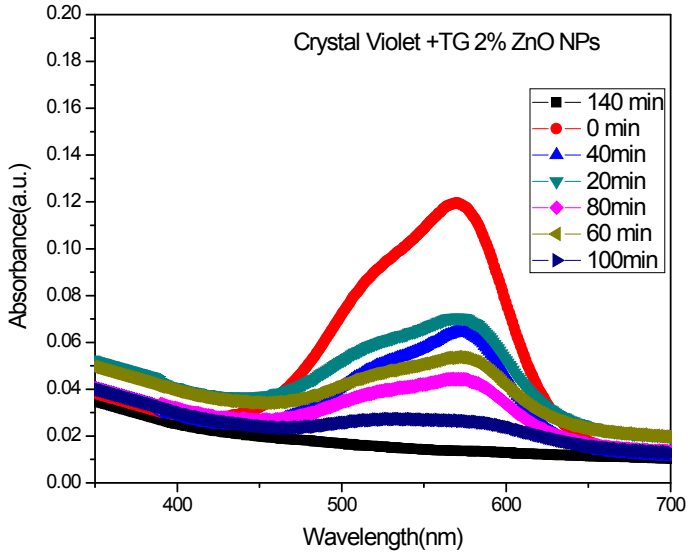

Fig. 5.5 Degradation of dye on addition of ZnO NPs

Chapter - 6

Conclusions

In this work, we have synthesized monodispersed ZnO nanoparticles with average size of 29 nm by chemical method with TG and ME as capping agent and double distilled water as solvent. The nanostructures of the prepared ZnO nanoparticles have been confirmed using UV-VIS absorption, XRD, and SEM micrograph analysis. The sharpness of the UV peak also shows that the ZnO nanoparticles size in these samples are nearly monodisperse. The PL emissions from the ZnO nanoparticles dispersed in water have been measured under 320 nm UV light excitations. The maximum PL emission has been observed covering the whole 350-550 nm visible region of the electromagnetic spectrum when 320 nm wavelengths are used for excitation. The strong green luminescence we observed, demonstrates the good quality of the prepared ZnO nanoparticles. As suggested and confirmed by others that such low energy emissions are assigned to the surface states. The density of surface states in the nanocrystals would increase with a decrease in the size of crystallites of the prepared nanocrystals, due to the increased surface-to-volume ratio having smaller crystallites. This would reduce the probability of excitonic emission via non-radiative surface recombination. The prepared ZnO NPs were also used as photocatalyst for breaking the organic pollutant i.e dye (crystal violet). The reduction in absorbance suggests that the dye molecules were completely mineralized along with color removal. It can be concluded that the ZnO assisted photocatalytic degradation of textile dyes may be a versatile, economic, and efficient method of treatment.

References

[1] http:/www.en.wikipedia.org

[2] http://www.tzhealth.com

[3] C.B. Murray, C.R. Kagan, M. G. Bawendi, **"Synthesis and Characterization of Monodisperse Nanocrystals and Close-Packed Nanocrystal Assemblies".** *Journal of Materials Research* **30** (2000) 545–610

[4] http://www.greentechgazette.com

[5] http://www.nist.govupdate/quantumdots.com

[6] Ying Chen, Chi Pui Li, Hua Chen and Yongjun Chen , "**One-dimensional nanomaterials synthesized using high-energy ball milling and annealing process"**, *Journal of Science and Technology of Advanced Materials,* **7 (**2006) 839

[7] http://www.ecotechdaily.com

[8] http://ucsdnews.ucsd.edu.science

[9] http://www. library.thinkquest.org

[10] http://www.en.wikipedia.org

[11] http://www.scitizen.com

[12] http://www.malvern.com

[13] https://www.ntt-review

[14] http://www.biologyjunction.com

[15] Murphy C.J., **"Nnanocubes and nanoboxes",** *Journal of Materials Science*, **298** (2002) 2139-2141

[16] http://www.Universe-review

[17] St. Charles, Illinois, **"Beam Laue Diffraction patterns",** American Conference on Neutron Scattering, (2006) 90-95, *Sponsored by the Neutron Scattering Society of America*

[18] Gregory Kalyuzhny, Alexander Vaskevich, Gonen Ashkenasy, Abraham Shanzer and Israel Rubinstein, **"UV/Vis Spectroscopy of Metalloporphyrin and Metallophthalocyanine Monolayers Self-Assembled on Ultrathin Gold Films",** *Journal of Physical Chemistry***, 104** (2000) 8238-8244

[19] Hao Zhang, Zhen Zhou and Bai Yang, **"The Influence of Carboxyl Groups on the Photoluminescence of Mercaptocarboxylic Acid-Stabilized CdTe Nanoparticles",** *Journal of Physical Chemistry,* **107** (2003) 8-13

[20] A.D Russell**, "Bacterial adaptation and resistance to antiseptics, disinfectants and preservatives is not a new phenomenon",** *Journal of Hospital Infection,* **57** (2004) 97–104

[21] Clemens Burda, Yongbing Lou, Xiaobo Chen, Anna C. S. Samia, John Stout, and James L. Gole, **"Enhanced Nitrogen Doping in TiO_2 Nanoparticles",** *Journal of Physical Sciences,* **3** (2003) 1049-1051

[22] Jayeeta Lahiri and Matthias Batzill, **"Surface Functionalization of ZnO Photocatalysts with Monolayer ZnS",** *Journal of Physical Sciences,* **112** (2008) 4304-4307

[23] Ashtaputre Shriwas S, Deshpande Aparna, Marathe Sonali, Wankhede M.E., Chimanpure Jayashree, Pasricha Renu, Urban J, Haram S.K., Gosawi S.W., Kulkarni S.K., **"Synthesis and analysis of ZnO and CdSe nanoparticles",** *Parmana***, 65** (2005) 615-620

[24] Radhouane Bel Hadj Tahar and Noureddine Bel Hadj Tahar**, "Boron-doped zinc oxide thin films prepared by sol-gel technique",** *Journal of Materials Science,* **40** (2005) 5285-5289

[25] Jiaguo Yu and Xiaoxiao Yu, **"Hydrothermal Synthesis and Photocatalytic Activity of Zinc Oxide Hollow Spheres",** *Journal of Enviornmental Science and Technology,* **42** (2008) 4902-4907

[26] Behnajady Mohammad A, Modirshahla Nasser, Shokri Mohammad, Zeininezhad Arezoo and Zamani Hassan A, **"Enhancement photocatalytic activity of ZnO nanoparticles by silver doping with optimization of photodeposition method parameters"**, *Journal of Enviornment Science and Health,* **44** (2009) 666-672

[27] Xue-lian Bai, Nan Pan, Xiao-ping Wang and Hai-qian Wang, "**Synthesis and Photocatalytic Activity of One-dimensional ZnO-Zn_2SnO_4 Mixed Oxide Nanowires**" *Chinese journal of chemical physics,* **21** (2008) 81-86

[28] Jozsef Nemeth, Geonel Rodrıguez-Gattorno, David Dıaz, America R. Vazquez-Olmos, and Imre Dekany, "**Synthesis of ZnO Nanoparticles on a Clay Mineral Surface in Dimethyl Sulfoxide Medium",** *Langmuir,* **20** (2004) 2855-2860

[29] Hiroyuki Usui, Yoshiki Shimizu, Takeshi Sasaki, and Naoto Koshizaki**, "Photoluminescence of ZnO nanoparticles produced by laser ablation method",** *J. Phys. Chem. B*, **109** (2005) 120–124

[30] K. Byrappa, A. K. Subramani, S. Ananda, K. M. Lokanatha Rai, R. Dinesh and M. Yoshimura, **"Photocatalytic degradation of rhodamine B dye using hydrothermally synthesized ZnO",** *Journal of Bulletin of Materials Science,* **29** (2008) 433-438

[31] Xu Ji-Chuan **"Photocatalytic activity of zinc ions surface doped TiO_2",** *Journal of Physical chemistry,* **108** (2004) 6004-6008

[32] S-M Zhu, J-Y Li, Y-S Li, Y Wang and Y-L Jiang, **"Reactive ion exchange synthesis of high purity ZnO nanoparticles",** *Journal of Nanoengineering and Nanosystems*, **221** (2009) 121-124

[33] Takuya Tsuzuki, Zoe Smith, Andrew Parker, Rongliang He and Xungai Wang, "**Photocatalytic Activity of Manganese-Doped ZnO Nanocrystalline Powders",** *Journal of the Australian Ceramic Society,* **45** (2009) 58-62

[34] Dodd A. McKinley A. Saunders M. and Tsuzuki T. **"Effect of Particle Size on the Photocatalytic Activity of Nanoparticulate Zinc Oxide",** *Journal of nanoparticle research*, **8** (2006) 43-51

[35] Manoj Sharma, Sunil Kumar and O. P. Pandey **"Study of energy transfer from capping agents to intrinsic vacancies/defects in passivated ZnS nanoparticles"**, *Journal of Nanoparticle Research,* 2010 DOI 10.1007/s11051-009-9844-2 (online)

[36] Manoj Sharma, Sunil Kumar and O.P.Pandey **"Photo-physical and morphological studies of organically passivated core-shell ZnS nanoparticles",** *Digest Journal of Nanomaterials and Biostructures,* **3** (2008) 189-197

[37] Manoj Sharma, Sukhvir Singh and O. P. pandey**, "Excitation induced tunable emission in biocompatible chitosan capped zns nanophosphors"**, *Journal of Applied Physics*, **107** (2010) 104319